AIR-WATER GAS EXCHANGE: MECHANISMS GOVERNING THE COMBINED EFFECTS OF WIND AND RAIN ON THE GAS TRANSFER VELOCITY AND FIELD MEASUREMENTS IN A EUTROPHIC REGION OF THE EVERGLADES OF THE EFFECTS OF WIND

A THESIS SUBMITTED TO THE GRADUATE DIVISION OF THE UNIVERSITY OF HAWAIʻI IN PARTIAL FULFILLMENT OF THE REQUIREMENTS FOR THE DEGREE OF

MASTER OF SCIENCE

IN

OCEANOGRAPHY

AUGUST 2011

By
Sarah Eggleston

Thesis Committee:

David Ho, Chairperson
Richard Zeebe
Geno Pawlak

We certify that we have read this thesis and that, in our opinion, it is satisfactory in scope and quality as a thesis for the degree of Master of Science in Oceanography.

THESIS COMMITTEE

Chairperson

Copyright 2011

by

Sarah Eggleston

ACKNOWLEDGMENTS

There are many people to whom I owe gratitude and without whom, this research would not have been completed. First and foremost, I would like to thank my advisor, Professor David Ho, for his willingness to take me as a student and for his support for the past two years. I also need to thank my committee members, Professors Richard Zeebe and Geno Pawlak, especially for their advice from how to operate instruments to suggestions for directions to go with my analysis.

Many people helped significantly in these experiments, especially Emily Harrison, at the University of Delaware, and her advisor and colleague Fabrice Veron and Marc Buckley. Wade McGillis and his group, including Philip Orton, Nadine Els, and Diana Hsueh, have been involved with many of the experiments at the Air-Sea Interaction Laboratory and have been a source of advice regarding data analysis for the present experiment. Matthew Reid and Kim Falinski were instrumental in helping me to sample during WRX 8. Professor Michael Sukop generously donated his lab space at the Florida International University for water sample analysis during the Everglades experiment presented here; Vic Engel was responsible for setting up a large amount of the equipment for the same experiment.

Once the data was collected, I would not have gotten far without the help of many people, including Mingxi Yang, Thomas Kilpatrick, and Tyson Hilmer, as well as many other colleagues at the University of Hawaii. Sara Ferrón has been extremely generous with her time over the past two years, editing drafts of proposals and chapters, and always willing to offer advice and a laugh.

Without encouragement from many friends, the writing process would have been significantly more painful. I especially need to thank everyone on board the RVIB Nathaniel B. Palmer during the CLIVAR S04P cruise, as well as Dana Erickson, Jennifer Murphy, Katharine Smith, Arisa Okazaki, Sherry Chou, Eunjung Kim, Christine Pequignet, and many others. Kathy Kozuma, Kristin Uyemura, Catalpa Kong, and Nancy Koike in the Ocean Office facilitated many things over the past two years, from ordering equipment to filing my petition to graduate.

Funding for the ASIL WRX experiments came from the National Science Foundation grant OCE 09-30057, Collaborative Research: Wind, waves, rain and

their effects on air-water gas and momentum exchanges. Funding for the Everglades experiment came from the United States Geological Survey, award #G1OAC00411.

Lastly, I would like to thank librarians at universities across the country for providing an unimaginable wealth of resources at my fingertips. I especially thank my parents for providing several of the papers I have cited here, and for their continued support for the past two and a half decades.

ABSTRACT

Air-water gas exchange is an important process in many biogeochemical cycles, including the global carbon cycle. Quantifying the movement of gases across the air-water interface is important to understand cycling on global and regional scales, to constrain the magnitude of the oceanic source or sink of biologically and climatically important trace gases, and to study local ecosystem dynamics. Although our knowledge of the mechanisms driving gas exchange due to individual processes, such as wind or rain, has improved greatly over the past few decades, there are regions where multiple processes may be significant in determining rates of gas exchange, and questions remain regarding the combined effects on the gas transfer velocity. Additionally, while many field studies have been conducted to measure gas exchange in a variety of environments, including lakes and wetlands, and to parameterize the gas transfer velocity in terms of its governing mechanisms and driving forces, the applicability of these parameterizations has not yet been established for all systems.

In the first study presented here, the mechanisms responsible for gas exchange under conditions of wind and rain were studied in the laboratory and quantified. Measured variables included turbulent kinetic energy, bubble formation frequency, wave slope, wind speed profiles and raindrop impact velocity, allowing calculation of the kinetic energy flux due to wind and rain. It was determined that the impact of rain on air-water gas exchange is significantly reduced at elevated wind speeds (12 - 20 m s^{-1} in this study). While this result differs quantitatively from two previous studies at the same facility, the findings can all be described by a model for gas exchange in which the gas transfer velocity depends on wind speed, u_{10}, and the excess mixing of rain beyond a critical depth of dissipation of TKE due to wind. This mixing is accounted for by taking into account depth scales relevant to rain and wind, z_R and z_u, which are assumed to scale by the kinetic energy fluxes of rain and wind, respectively. The parameterization $k_{600} = au_{10}^2 + b(\mathrm{KEF}_{\mathrm{rain}} - c\mathrm{KEF}_{\mathrm{wind}})^{\beta}$ describes the results from each of the two previous studies as well as the present study. While this model predicts that the effect of rain would be negligible in high-wind, low-rain regions of the oceans such as the Southern Ocean, rain may be very important to take into account in regions with characteristically high rain rates and low wind speeds.

Our second study focused on field measurements of gas exchange in the Everglades, where the effect of vegetation on the gas transfer velocity was measured, in terms of emergent macrophytes impacting the wind profile. It was determined that vegetation may have an impact on the wind profile comparing measurements at 85 cm and 10 m above the water surface, and common parameterizations for k_{600} as a function of u_{10} derived from experiments on oligotrophic lakes such as that proposed by Cole and Caraco (1998) over-predict the gas transfer velocity by as much as 300% in a eutrophic wetland region such as the degraded ridge and slough environment found in the Everglades. This has important implications for biological studies in such regions that use parameterizations for the gas transfer velocity in calculating metabolic rates.

Contents

List of Tables **x**

List of Figures **xi**

1 Introduction **1**
1.1 Previous studies 4
1.2 Objectives 7

2 Wind, Rain, and Gas Exchange: Results from the laboratory **9**
2.1 Introduction 9
2.2 Methods 12
2.2.1 Air-Sea Interaction Laboratory 12
2.2.2 Experimental design 13
2.2.3 Wind speed 13
2.2.4 Rain rate 14
2.2.5 Turbulence 16
2.2.6 Bubbles 16
2.2.7 Wave slope 17
2.2.8 Gas tracer experiments 17
2.2.9 Gas evasion technique and calculations 18
2.3 Results 20
2.3.1 Wind 20
2.3.2 Rain 20
2.3.3 Kinetic energy flux 21
2.3.4 Turbulence and bubbles 21
2.3.5 Wave slope 23
2.3.6 Gas transfer velocities from SF_6 23
2.4 Discussion 24
2.4.1 Kinetic energy flux 24
2.4.2 Gas transfer velocity 25
2.4.3 Turbulence 32
2.4.4 Wave slope 33
2.5 Summary and Conclusions 34

3 Gas Exchange in a Ridge and Slough Region in the Everglades 48
3.1 Introduction 48
3.2 Methods 51
3.2.1 Everglades research site 51
3.2.2 Environmental parameters 53
3.2.3 Gas tracer experiments 54
3.3 Results 55
3.3.1 Atmospheric stability 55
3.3.2 Wind speeds 55
3.3.3 Gas transfer velocities 57
3.3.4 Effects of periphyton on gas exchange 58
3.4 Discussion 59
3.4.1 Sawgrass and wind speed profile 59
3.4.2 Gas transfer velocity parameterization 61
3.5 Summary and Conclusions 63

List of Tables

2.1 Summary of Wind-Rain eXperiments (WRX) conducted at the Air-Sea Interaction Laboratory, 2005 - 2010 45

2.2 Results of gas exchange experiments using 23g hypodermic needles in rain modules 46

2.3 Results of gas exchange experiments using 20g hypodermic needles in rain modules 47

2.4 Comparison of results from gas transfer velocity experiments in the laboratory to determine the dependence of k_{600} on fetch; k_{600} is larger at comparable wind speeds in tanks with larger fetch by the percentage indicated here 47

2.5 Application to the field: Typical conditions in the Everglades and associated gas transfer velocities assuming (a) no effect of rain, (b) linearly additive effects of wind and rain, (c) relationship presented in Equation 2.4.8 47

3.1 Atmospheric parameters (averaged) and gas transfer velocities measured throughout experiment; 10-m wind speed was measured at station S331W and the extrapolated u_{10} is derived from the 85-cm wind speed measurements and the COARE algorithm 69

List of Figures

2.1 Small wind-wave-current tank used for gas exchange experiments in WRX 8; diagram created by Emily Harrison and Marc Buckley . . . 36
2.2 Example of wind speeds above the water surface and interpolated logarithmic wind speed profile from WRX 8, experiment 32 37
2.3 Kinetic energy flux of rain and wind impacting the water surface . . . 37
2.4 Turbulence density spectra in three dimensions, experiment 13. Green line shows -5/3 slope 38
2.5 Turbulent kinetic energy as a function of wind speed and rain rate . . 38
2.6 Sample image of bubble forming at air-water interface 39
2.7 Frequency of bubble formation as a function of rain rate and wind speed. Solid line shows trend in frequency at lowest rain rate (8.1 - 12.1 mm h^{-1}), though slope is not significantly different from 0 at 95% confidence level 39
2.8 Wave slope spectra grouped by wind speed; no rain (black), low rain rate (red), medium rain rate (green), high rain rate (blue). At wind speeds below 14 m s^{-1}, the spectral power densities for rain and no-rain cases show distinct frequencies of peak wave slopes. The spectra are indistinguishable for our purposes at wind speeds of 14 m s^{-1} and above, signifying the reduced effects of rain on the wave slope at this wind speed 40
2.9 Gas transfer velocities measured in WRX 8; solid line shows parameterization for k_{600} as a quadratic function of the 10-m wind speed . . 41
2.10 Gas transfer velocity from no-wind experiments parameterized as a function of the the kinetic energy flux of rain 41
2.11 Comparison of k_{600} measured in all WRX 8 experiments to gas transfer velocities derived from a parameterization of the functional form in Equation 2.4.6 42
2.12 Comparison of k_{600} measured in all WRX 8 experiments to gas transfer velocities derived from a parameterization of the functional form in Equation 2.4.7 42
2.13 Comparison of k_{600} measured in all WRX 3 (Harrison *et al.*, in prep) experiments to gas transfer velocities derived from a parameterization of the functional form in Equation 2.4.7 43

2.14 Comparison of gas transfer velocities predicted by linearly additive model (Equation 2.4.6; dashed lines) and mixing depth model proposed here (solid lines; Equation 2.4.7) 43
2.15 Net annual effect of rain on the CO_2 gas flux in the tropics, expressed as a percentage of total gas flux. Here, only the effect of rain on the gas transfer velocity is taken into account; the dependence of the interfacial CO_2 gradient is neglected 44

3.1 Platform, one limnocorral, and tripod with anemometers (85 cm and 3.0 m above water level) used in present experiment 65
3.2 Air and water temperature and relative humidity over the course of the experiment 66
3.3 Wind speeds measured at a nearby meteorological station (S331W) at 10 m and at the study site at 85 cm above the water surface 67
3.4 An idealized wind speed profile near the sawgrass based on the true 10-m wind speed during Day 1 compared to the extrapolated wind speed profile based on the 85-cm wind speed and the COARE algorithm; highlight points show measured wind speeds 67
3.5 Gas transfer velocities measured in limnocorrals 1 and 2 over the four days of the experiment. Error bars show standard error for each calculated value 68
3.6 Gas transfer velocity plotted against 10-m wind speed, measured at station S331W. Common parameterizations are shown predicting gas transfer velocity from the 10-m wind speed, including a best-fit parameterization for the present data (red line) 68

Chapter 1

Introduction

Air-water gas exchange is an important process to understand in order to quantify global and local biogeochemical cycling of biologically and climatically important trace gases including CO_2, CH_3, N_2O, DMS, and CH_3Br (Broecker *et al.*, 1985; Bates *et al.*, 1993; Yvon and Butler, 1996; Forster *et al.*, 2007). It is also necessary to know the magnitude of the air-water flux to determine the fate of volatile pollutants, such as polychlorinated biphenyls (PCBs), hexachlorocyclohexanes (HCHs), tetrachloroethane (PER), atrazine, and nitrilotriacetate (NTA) (Bopp, 1983; Thomann *et al.*, 1991; McConnell *et al.*, 1993; Ulrich *et al.*, 1994). Although research in this field was initially driven by industrial demands (e.g. Higbie, 1935; Danckwerts, 1970), results from these studies have informed more recent environmental research. Over the past few decades, much research has been focused on better understanding the mechanisms behind air-water gas exchange, parameterizing the gas transfer velocity in terms of easily measured variables, and applying this work to biological and chemical studies in the upper ocean (e.g. Asher and Pankow, 1986; Asher *et al.*, 1997; Ho *et al.*, 2000; Liss and Merlivat, 1986; Wanninkhof, 1992; Takahashi *et al.*, 2009). As a result, our understanding of both the mechanisms responsible for gas exchange and the mathematical dependence of gas exchange on individual driving processes including wind and rain have been remarkably improved as of late.

Air-water gas flux is controlled by the gas transfer velocity, k, and the concentration of the gas in the bulk fluid, C_b, compared to the concentration at the water

surface, C_0:

$$F = k(C_b - C_0) \tag{1.0.1}$$

The difference in gas concentration is controlled by a myriad of processes; in the case of biologically active gases such as CO_2 or O_2, this is influenced by photosynthesis and respiration as well as chemical and physical processes, including chemical speciation, calcification and dissolution, advection, dispersion, and gas exchange (Odum, 1956; Caffrey, 2004). Although measurements of ΔpCO_2 are becoming more routine (e.g. Takahashi *et al.*, 2002, 2009) and accurate (Pierrot *et al.*, 2009), the uncertainty in global flux estimates due to the number and accuracy of these data remains significant, estimated at 13% (Takahashi *et al.*, 2009). This is an important topic to address in calculating global gas fluxes, but discussion of these measurements and analysis is beyond the scope of this thesis. It has been shown that a parameterization for the gas transfer velocity in terms of wind speed alone can account for 80% of the variance in data from a large range of oceanic and coastal gas exchange studies (Ho *et al.*, 2011b). However, there are regions in which multiple processes, such as wind and rain, can be important to mediating gas exchange (e.g. Turk *et al.*, 2010), and it is not yet fully understood how the interaction of these processes affects near-surface turbulence and the gas transfer velocity. Additionally, in regions such as lakes or wetlands, wind may not be the main process governing gas exchange, so it is important to constrain the gas transfer velocity in such regions. Henceforth, we focus on the gas transfer velocity as a constraint on the magnitude of the gas flux.

There are currently several different techniques used to measure gas exchange on a range of timescales, including micrometeorological techniques, which measure gas exchange over timescales of minutes to hours, and tracer methods, with timescales of hours to days to decades. Of the micrometeorological techniques employed, direct covariance and atmospheric profiling are discussed here. Direct covariance makes use of high-frequency measurements of vertical velocity and gas concentration in the atmospheric boundary layer in determining the gas flux (Businger *et al.*, 1971; Jones and Smith, 1977). Using this technique at sea presents some technical difficulties, including correcting for the movement of the ship (e.g. Fairall *et al.*, 1997) and making rapid measurements of gas concentration which may result in low

signal-to-noise ratios, necessitating averaging fluxes over periods on the order of 30 minutes (e.g. McGillis *et al.*, 2001). The atmospheric profile method, based on Monin-Obukhov (MO) similarity theory (Monin and Obukhov, 1954; Panofsky and Dutton, 1984), is advantageous in not requiring high-frequency gas measurements. However, this method requires knowledge of the flux profile and a dimensionless constant, ψ, which can be determined if the MO length or the gas transfer velocity is known (e.g. McGillis *et al.*, 2001; Ho *et al.*, 2007). When the gas transfer velocity is unknown, one must rely on calculating the MO length, requiring parameterizations for buoyancy fluxes, for example, that have historically been made over land (e.g. Businger *et al.*, 1971). The relative merits and difficulties with these methods are described in more detail by McGillis *et al.* (2001) and Wanninkhof *et al.* (2009).

A number of tracer techniques have been employed in measuring gas exchange in the laboratory as well as in the field, utilizing natural and opportunistic, or deliberately injected tracers. Of the natural and opportunistic tracers, radon (^{222}Rn) profiles in the surface ocean have been used to calculate the gas transfer velocity (e.g. Broecker and Peng, 1971). Additionally, long-term global average gas transfer velocities can be estimated from natural or bomb-produced ^{14}C (Broecker *et al.*, 1985; Naegler *et al.*, 2006; Sweeney *et al.*, 2007). The deliberate tracer technique (e.g. Tsivoglou *et al.*, 1968; Rathbun, 1979; Wilcock, 1984; Jähne *et al.*, 1985; Wanninkhof *et al.*, 1985) employs a biologically and chemically inert gas which is naturally present in the water and atmosphere in very low concentrations but can be measured analytically to a high precision, such as sulfur hexafluoride (SF_6). A quantity of the tracer gas is injected into the water, and the waterside and airside concentrations of the gas are measured over time, allowing calculation of the gas evasion rate using a mass-balance equation for the gas of interest. In oceanic studies, gas dilution due to advection and dispersion of the water parcel where the gas is injected make it necessary to use two gas tracers to calculate the gas exchange (dual-tracer method). In this method, two gases with significantly different diffusivities (e.g., SF_6 and ^{3}He) are injected into the water at a constant ratio, and the change in that ratio is measured over time to calculate the gas transfer velocity (Watson *et al.*, 1991; Wanninkhof *et al.*, 1993). The SF_6 deliberate tracer technique is the method employed in the studies

discussed below and the present experiments described in more detail in Chapters 2 and 3.

Because of widespread interest in climate change and hence studying gas exchange on a global scale, as well as in knowing the gas flux in regional studies where it is not always feasible to measure the gas transfer velocity directly, it is common to parameterize the transfer velocity in terms of the governing processes of gas exchange. Air-water gas exchange is governed primarily by turbulence near the water surface, which in turn is driven primarily by wind. As a result, many parameterizations have been developed from the results of field or laboratory studies, relating the gas transfer velocity to wind speed (e.g. Liss and Merlivat, 1986; Wanninkhof, 1992; Wanninkhof and McGillis, 1999; Nightingale *et al.*, 2000; Ho *et al.*, 2006). Furthermore, it has been established that wind most likely accounts for at least 80% of gas exchange in both coastal and oceanic regions (Ho *et al.*, 2011b). Some of the influential studies that have contributed to our understanding of this relationship and the dependence of the gas transfer velocity on other variables are discussed below.

1.1 Previous studies

Many wind tunnel studies (see, for instance, Borges and Wanninkhof, 2007; Wanninkhof *et al.*, 2009, and references therein) have been conducted in the laboratory to investigate the dependence of the gas transfer velocity on wind. These studies are highly beneficial in understanding gas exchange from a mechanistic standpoint and can inform further studies in the field by identifying relevant mechanisms and processes that enhance or dampen air-water gas exchange. Although it has been established that the gas transfer velocity is fetch-dependent (Jähne *et al.*, 1989; Wanninkhof, 1992) and therefore probably underestimated by wind tunnel studies, these initial measurements were coupled with results from lakes experiments, leading to one of the first widely-used parameterizations (Liss and Merlivat, 1986). An approach using the long-term global oceanic natural and bomb-produced radiocarbon invasion led to the most commonly used parameterization today (Wanninkhof, 1992); the average gas transfer velocities and wind speeds from the Red Sea and the global oceans

(Broecker *et al.*, 1985; Cember, 1989; Naegler *et al.*, 2006; Sweeney *et al.*, 2007) have been used to constrain all subsequently proposed parameterizations.

Further field experiments in lakes and oceanic regions (e.g. Cole and Caraco, 1998; Nightingale *et al.*, 2000; Ho *et al.*, 2006) have since led to a number of different parameterizations for gas exchange. While it has been determined that a single parameterization can be used to account for the spread of data from oceanic studies (Ho *et al.*, 2011b) as well as other environments including the Hudson River, a tidal estuary (Ho *et al.*, 2011a), it is possible that this parameterization may not apply to regions with characteristically low wind speeds, such as lakes and wetlands. The wind speed range is important as the gas transfer velocity is typically believed to be independent of wind below approximately 3 m s^{-1}; in this range, k may be related more closely to buoyancy fluxes (Livingstone and Imboden, 1993; Soloviev and Schlüssel, 1994; Clark *et al.*, 1995). The wind fetch is also important to the development of waves and turbulence (Jähne *et al.*, 1989; Wanninkhof, 1992), and this variable can change significantly between lake and oceanic regions. It is important to note that differences in gas exchange data from different environments may depend largely on the experimental technique employed (Ho *et al.*, 2011a). Historically, however, separate parameterizations have been developed from experiments in lakes, rivers, estuaries, and marine systems based on differences in the governing processes of gas exchange in each of these environments.

Although it has been established that wind is the most important process driving air-sea gas exchange, other processes can play a role in low-wind speed environments, including rain (Banks *et al.*, 1984; Ho *et al.*, 1997, 2000; Takagaki and Komori, 2007; Turk *et al.*, 2010). Laboratory results from these studies showed that, in the absence of wind, the gas transfer velocity can be parameterized as a function of the kinetic energy flux of rain. Further experiments in the lab allowed the mechanisms responsible for this gas exchange enhancement to be quantified (Ho *et al.*, 2000). These data indicated that gas exchange enhancement of SF_6 due to a kinetic energy flux of 0.45 J m^{-2} s^{-1} (corresponding to a natural rain rate of 65 mm h^{-1}, assuming the kinetic energy flux and natural rain rate relationship derived by Ho *et al.* (1997)) was approximately 11% bubble-mediated, with turbulence accounting

for the remaining 89%. Sulfur hexafluoride is a highly insoluble gas and therefore more affected by bubbles than other, more soluble gases (Ho *et al.*, 2000). Experiments at Biosphere 2 investigating the impact of rain on gas exchange in saltwater demonstrated that while the flux differs from the freshwater case due to the formation of a freshwater lens at the water surface, affecting the gas concentration profile, the gas transfer velocity is not significantly affected by the salinity (Ho *et al.*, 2004), although the bubble-mediated portion of k is lower in saltwater due to the formation of fewer large bubbles (Asher *et al.*, 1997).

It has been established, too, that surface active materials, or surfactants, affect air-water gas exchange (Broecker *et al.*, 1978; Asher and Pankow, 1986; Frew *et al.*, 1990, 2004; Bock *et al.*, 1999; Saylor and Handler, 1999). Laboratory experiments conducted by Frew *et al.* (1990) utilized phytoplankton known to produce certain organic compounds that act as surfactants to show that the gas transfer velocity was diminished by 5 - 50% in experimental runs. This reduction in gas evasion is explained by a reduction of turbulence in the surface water, particularly affecting microscale breaking waves, the scale of interest in gas transfer (Csanady, 1990; Zappa *et al.*, 2001).

Through buoy measurements and modeling, it has been shown that in some regions with characteristically low wind speeds, the effect of rain may be significant in comparison to that of wind (Turk *et al.*, 2010). Therefore, for this type of environment, it is of interest to study the two processes in tandem. Dynamics experiments have examined the physical interactions of rain and waves; Tsimplis and Thorpe (1989) determined that while rain may enhance turbulence on a capillary-wave scale, waves with longer wavelengths are damped in the presence of rain. Poon *et al.* (1992) examined the interactions of rain and waves in the presence of wind, where a similar result was found, but at the highest wind speed (6.34 m s^{-1}), rain had a negligible effect on the water surface ripple structure. Very few laboratory experiments to date have coupled dynamics experiments with gas exchange experiments to examine combined effects of wind and rain on gas exchange. The first experiments to do so were conducted at the Air-Sea Interaction Laboratory at the University of Delaware in March 2005 (Ho *et al.*, 2007), where it was determined from initial experiments

that the effects of wind and rain on gas exchange were linearly additive. It was recognized, however, that this result may have been due to the experimental setup: the tank was not sealed at the top, precluding high wind speeds from experimental conditions. Additionally, a single rain module covering approximately 4% of the tank surface area was used to generate raindrops; this may have given the rain and wind insufficient volume over which to interact. Further experiments at the same facility indicated that at wind speeds above 12 m s^{-1} with rain modules covering 50% of the tank surface, the effect of rain on gas exchange is negligible (Harrison *et al.*, in prep). Several more experiments have been conducted to examine these results in more detail and to gain a better understanding of the mechanisms responsible for the gas transfer velocities that were measured. A discussion of each of these experiments and the present study is given below (Chapter 2).

1.2 Objectives

Below, we present results from two sets of experiments, one from the laboratory and one from the field. The first is a series of experiments conducted as a continuation of a several wind-rain experiments at the Air-Sea Interaction Laboratory at the University of Delaware. The first goal of these experiments is to reconcile the apparently contradictory results of previous studies. Secondly, we aim to gain a better understanding of the mechanisms responsible for the trends in gas transfer velocities that we measured under a wide variety of combined wind and rain conditions. We present a parameterization describing our results quantitatively, to account for the gas exchange due to wind and rain. The coefficients derived from this study may not be applicable to gas exchange in nature due to the tank specifications, such as the fetch, and the specific tank dynamics: for example, additional turbulence may be introduced by reflecting waves. However, the functionality of the parameterization can easily be applied to field studies, as demonstrated within the chapter.

The second set of gas exchange experiments presented here was carried out at a field site in a eutrophic region of the Florida Everglades. The Everglades is a unique environment and one of great interest in studying ecosystem dynamics, so it

is important that gas fluxes are well-constrained in these studies. Additionally, it is likely that published gas transfer velocity parameterizations may not be applicable to this environment due to the short fetch, low wind speeds, abundance of biology and surface films, and vegetation extending above the water surface that may influence the wind profile in certain regions. The purpose of this experiment was threefold: first, to compare the gas transfer velocities measured to those that would be predicted by commonly used parameterizations for gas exchange, including Cole and Caraco (1998). The second goal of the experiment was to examine the effect of a physical obstruction to the wind field near the water surface on gas exchange: sawgrass extends above the water surface, therefore impacting the wind field and hence affecting turbulence and gas exchange. Finally, we attempted to quantitatively constrain the effect of biology on gas exchange. Periphyton, in the water, floats at the surface and provides a barrier to air-water gas transfer; reduces near-surface turbulence; and produces surfactants, which have been found to reduce gas transfer as well. However, in the present study, we were not able to quantify this effect on gas exchange, as discussed below.

Overall, we aim to provide an understanding of some of the important mechanisms that should be considered in parameterizing air-water gas exchange in low-wind speed regions where rain is prevalent. Results from a field study are also presented; we compare the data to existing parameterizations for gas exchange on lakes and wetlands, as parameterizing gas exchange accurately is important in constraining local biogeochemical cycles.

Chapter 2

Wind, Rain, and Gas Exchange: Results from the laboratory

2.1 Introduction

Air-water gas exchange is governed primarily by turbulence near the interface. Turbulence is, in turn, controlled by the natural phenomena of wind and rain. While many previous experiments have investigated the effects of these two variables on gas exchange separately (e.g. Liss, 1983; Wanninkhof *et al.*, 1985; Banks *et al.*, 1984; Ho *et al.*, 1997), only recently have studies begun to examine the combined effects of wind and rain on gas exchange (Ho *et al.*, 2007; Harrison *et al.*, in prep). Although the mechanisms governing gas exchange are well understood in terms of enhancement due to wind and rain separately, it is not yet well known how the interactions of these two driving forces affect air-water gas exchange. Each of these processes enhances gas exchange primarily through increasing near-surface turbulence, though wind exerts a shear stress on the water surface, while rain impacts the water more or less perpendicularly. Bubbles also play a role in enhancing gas transfer, particularly in the case of sparingly soluble gases (Merlivat and Memery, 1983; Farmer *et al.*, 1993; Asher *et al.*, 1996; Ho *et al.*, 2000). Results from recent experiments have shown that the effects of wind and rain on gas exchange are not linearly additive (Harrison *et al.*, in prep); here, we strive to understand the interaction of wind and rain and the subsequent effect on gas exchange mechanistically.

The first gas exchange studies designed to examine the combined effects of wind and rain on gas exchange were conducted in a wind-wave-current tank at the Air-Sea Interaction Laboratory (ASIL) at the University of Delaware's College of Earth, Ocean, and Environment in March 2005. Multiple techniques were employed to measure the gas transfer velocity during Wind-Rain eXperiment (WRX) 1, including the deliberate tracer gas evasion technique (described in more detail below). A single rain module containing 6922 20-gauge hypodermic needles was used in the experiments, which covered approximately 4% of the water surface in the tank. This resulted in a small space over which rain and wind were able to interact before the raindrops impacted the surface, as well as relatively low tank-averaged rain rates. Twelve gas exchange experiments were conducted in total, in which wind speeds ranged from 0 - 13 m s^{-1} and rain rates were 0 - 26 mm h^{-1}. Results from this study indicated that the effects of wind and rain on the gas transfer velocity were linearly additive (Ho *et al.*, 2007). This did not fall in line with the hypothesis for the experiment, as previous laboratory studies investigating the dynamics of wind/rain interactions have demonstrated that wind waves, the primary mechanism for wind-enhancement of gas exchange, are damped by rain (Tsimplis and Thorpe, 1989; Poon *et al.*, 1992). To examine if the experimental setup or the range of wind speeds and rain rates might have been responsible for this result, seven rain modules were added to the tank; technical considerations required lowering the rain modules from 2.6 m to approximately 65 cm above the water level. WRX 2 and 3 were conducted at the same facility in 2008. During WRX 3, 27 experiments were carried out, and the maximum wind speed and rain rate were increased to 19 m s^{-1} and 62 mm h^{-1}, respectively. These results illustrated that the effects of wind and rain on air-water gas exchange are not linearly additive; indeed, at wind speeds above 12 m s^{-1} in this experimental setup, the effect of rain was negligible (Harrison *et al.*, in prep).

Further gas exchange experiments were conducted at the ASIL to examine the combined effects of wind and rain on gas exchange in more detail (WRX 4). It was found that, although the wind speed and rain rate ranges were similar to WRX 3, comparable conditions yielded lower gas transfer velocities during WRX 4. Prior to this experiment, holes in the rain modules on the tank had been caulked,

and it was hypothesized that the caulking may have caused rainwater to transport surfactants from the modules to the tank, thus reducing gas exchange. In 2009, a second wind-wave-current tank was constructed at the facility, made of clear plastic, therefore allowing future experiments to compare the combined effects of wind and rain on gas exchange in saltwater. As in WRX 1, a single rain module was installed above the tank; however, the module was raised 5 m above the water level, allowing raindrops to reach near terminal velocity, and the wind generator was capable of wind speeds up to 21 m s^{-1}. Pilot experiments were conducted in the small tank in June 2009 using freshwater (WRX 5). In July 2010, WRX 6 was conducted in the larger tank to examine differences between results in WRX 3 and 4 and to investigate the effect of rain on surfactants in the tank by measuring surface tension and gas transfer velocities before, during, and after rain events. Results were not conclusive, however, as no significant difference in the gas transfer velocity was found at a given wind speed before and after experiments with rain. In August 2010, WRX 7 and 8 were conducted in the smaller tank at the ASIL using freshwater and a single rain module, as in WRX 1, to gather a full suite of gas exchange data at a range of wind speeds and rain rates similar to WRX 3. The above experiments are summarized in Table 2.1. Here, we present results from WRX 8.

Although previous experiments at the ASIL had determined gas transfer velocities at a number of wind speed and rain rate conditions and measured some ancillary parameters including wave height and kinetic energy flux due to wind and rain in efforts to conceptualize a model for gas exchange under these conditions, results were seemingly contradictory. While data from WRX 1 suggested that the effects of wind and rain on gas exchange may be linearly additive, results from WRX 3 demonstrated that this was not the case. The goal of WRX 8 was to reconcile these results by conducting experiments with wind speeds and rain rates similar to WRX 3 but using a tank setup similar to that of WRX 1. During WRX 8, instruments were deployed to measure the near-surface turbulence and frequency of bubble production due to rain. Additionally, factors that are affected by both wind and rain, including kinetic energy flux and the wave slope spectra, were calculated from measurements of wind speed profiles, raindrop impact velocities, and wave slope in order to relate

the physical interactions between wind and rain to the corresponding gas transfer velocities. Technical problems were encountered in collecting turbulence and bubble frequency data, so we focus on the kinetic energy flux, wave slope, and the gas transfer velocities in our discussion. We compare the effects of wind and rain on the air-water interface in terms of the kinetic energy flux due to each process as well as the associated mixing depth with respect to gas in the water.

In the following section, we introduce the facility and the experimental setup, as well as the methods used in measuring each of the parameters monitored in these experiments. We present our results from these experiments in Section 3, followed by our discussion and synthesis of the results in Section 4, where we present a physical and quantitative description of our data and propose a mechanism to understand the observations based on a comparison of the depth of mixing by raindrops and the depth of significant dissipation turbulent kinetic energy due to wind. We conclude with a summary and final remarks in Section 5.

2.2 Methods

2.2.1 Air-Sea Interaction Laboratory

Located at the University of Delaware's College of Earth, Ocean, and Environment, the ASIL houses two wind-wave-current tanks, each equipped with modules to simulate rain. The present gas exchange experiments constituted the WRX 8 campaign and were conducted in the smaller of the two tanks, which provides a wind fetch of approximately 7 m and, with the exception of the stabilizing metal frame, is constructed of clear plastic (see Figure 2.1). A plastic beach at the downwind end of the tank squelches waves to eliminate standing wave effects. Three submerged recirculating pumps were installed for the present experiment to ensure that the water remained well-mixed with respect to the tracer gas. The pump intake was located under the beach, and the water was pumped to the bottom of the tank below the wind generator. A single rain module was installed 5 m above the tank. Rain water was stored in tanks at ground-level and continuously aerated to ensure that it was in

equilibrium with the atmosphere. Pumps transported the water to a holding tank, where it was then released during experiments through the rain module. Six different rain modules were used throughout WRX 8 to control the rain rate by varying the number and gauge of the hypodermic needles in each module. Three modules contained 23g needles, while the other three contained 20g needles and were used only for experiments 42 - 44.

2.2.2 Experimental design

During WRX 8, 44 experiments were conducted at a variety of wind speeds ($u_{10} \in [0, 20.9]$ m s^{-1}) and rain rates ($R \in [0, 45.6]$ mm h^{-1}). Because this was the first complete set of gas exchange experiments conducted in this tank, 21 of the experiments were conducted under wind-only conditions to obtain a robust parameterization for the gas transfer velocity, k, in terms of wind speed. Of these, 15 experiments comprised 5 distinct wind conditions run in triplicate to determine the accuracy of the data, and the six remaining experiments were conducted at intermediate wind speeds. Six experiments were conducted with rain only to derive a relationship between k and the kinetic energy flux due to rain (this calculation is discussed below). The remaining experiments were conducted at various wind speeds and rain rates, enabling quantification of the combined effects of wind and rain on the gas transfer velocity.

The water depth in the tank was maintained at 40.0 cm. The mean water temperature was 21.5^o C (standard deviation 0.8^o C), and there was no significant gradient throughout the tank.

2.2.3 Wind speed

A pitot tube, measuring the difference between the total and static air pressures, was used to determine wind speeds near the water surface during each experiment. The instrument was located upwind of the rain module to avoid possible flooding during high wind and rain events. To obtain an accurate wind profile in the vicinity of the air-water interface, wind speeds were measured at 6 heights above the

surface between 2 and 8 cm; heights were varied based on the wave field at each wind speed. Wind speeds were determined at each height by sampling the air pressure for 8 minutes; the cycle was then repeated to ascertain that the wind field was established and stable.

Friction velocity and kinetic energy flux

Wind speed profiles were estimated assuming a logarithmic profile and assuming neutral atmospheric stability:

$$U(z) = \frac{u_*}{\kappa} \ln\left(\frac{z}{z_0}\right) \tag{2.2.1}$$

where κ is the von Kármán constant ($\kappa \approx 0.4$), u_* is the friction velocity, and z_0 is the roughness length. Both u_* and z_0 were calculated for each experiment based on the best-fit coefficients for the measured wind profile, where u_*/κ is given by the slope and z_0 is determined from the intercept.

The kinetic energy flux of wind was calculated from the density of air (ρ_a) and friction velocity:

$$\mathrm{KEF}_{\mathrm{wind}} = \rho_a u_*^3 \tag{2.2.2}$$

2.2.4 Rain rate

The depth of the water in the tank was maintained at a constant level throughout each experiment by pumping water out of the tank from below the beach. The pumping rate had been calibrated so that the volume per unit time was well known. The total amount of time that the pumps remained on for each experiment was recorded and used to calculate the depth-rain rate (mm h^{-1}). Because a single rain module, which covered approximately 17% of the water surface, was employed during each experiment, the measured rain rates represent the tank average rainfall over the course of the experiment. Thus, the highest rain rate, 45.6 mm h^{-1}, represents a local rain rate of approximately 274 mm h^{-1}.

Raindrop impact velocity and kinetic energy flux

Because each rain module consisted of only one size of hypodermic needle, we assume that the raindrop diameter is constant for our purposes. A sample dropsize distribution from such a module was reported by Ho *et al.* (2007). The raindrop diameter affects the rain rate, as this is a measure of the total amount of water falling over an area in a given amount of time; the impact velocity, as larger raindrops have greater mass and therefore fall faster than smaller raindrops; and the size of bubbles formed as a consequence of impinging raindrops. Although we were not able to quantify the size of the bubbles formed in these experiments, the size of the bubbles can be important in affecting gas exchange (Asher *et al.*, 1996; Ho *et al.*, 2000). We are not able to determine the significance of the raindrop size to the gas transfer velocity in this thesis, so this element is not discussed further. The total gas transfer velocity induced by rain, however, has been found to be a function of the kinetic energy flux; in calculating the KEF due to rain, it is necessary to measure both the rain rate and the raindrop impact velocity. To determine the horizontal and vertical impact velocities at each wind speed, images from a high-speed camera operating at 1000 Hz were analyzed for raindrop speed in two dimensions. For each experiment, the velocity of at least 30 droplets within 5 cm of the water surface was measured and averaged.

In a laboratory setup with a single raindrop size, the kinetic energy flux was thus computed from the density of the raindrops (ρ_w), depth rain rate (R), and impact velocity of the raindrops (v_{im}), derived by Ho *et al.* (1997):

$$\mathrm{KEF}_{\mathrm{rain}} = \frac{1}{2}\rho_w R v_{im}^2 \tag{2.2.3}$$

In the analysis and discussion below, we assume that the mixing depth due to rain is proportional to the kinetic energy flux (Green and Houk, 1979). This is based on the results of an experiment investigating air-water heat transfer under different rain conditions, so there are limitations to this assumption. However, this same approach could be used if another parameter is found to scale better with the mixing depth due to rain with respect to gas exchange in future experiments.

2.2.5 Turbulence

An acoustic Doppler velocimeter (Nortek Vectrino) was used to measure turbulence in the water. The ADV measures three-dimensional water flow by measuring the Doppler effect of sound emitted from the instrument and reflected off of particles in the water, so 14-μm glass beads were added to the tank water and allowed to mix just before each experiment began to ensure a high signal-to-noise ratio. The ADV faced upward, and the transducer was located 10 cm below the water surface; the maximum wave height at the highest wind speed was 4 cm. The instrument sampled at its maximum frequency of 25 Hz with a nominal velocity range of $\pm$ 30 cm s^{-1} and a transmit length of 1.8 mm. Spectra of the u, v, and w velocity data were calculated over a 30-minute period after the flow fields had been established and stabilized using 33-sec Hanning windows and 50% overlap on each side, and turbulent kinetic energy (TKE) values were calculated by integrating the spectra along a common frequency domain for the turbulent regime. Due to significant noise in the spectra, however, we do not provide a detailed quantitative analysis of the results with respect to the relationship between TKE and the gas transfer velocity. The reason for noise in the spectra is postulated in the results section below.

2.2.6 Bubbles

A second high-speed camera imaging the air-water interface captured images of bubbles formed by raindrops impinging on the water. The approximate depth range for images was 2 cm. As the average hue intensity of the images typically grew darker over the course of each experiment, a single intensity cutoff could not be selected to differentiate air from water; therefore, the trough between the peaks of light and dark intensities was chosen for each image to differentiate between air and water. At least 310 images from each experiment in which the rain rate was nonzero were analyzed to compare the frequency of bubble formation. Seven different sets of images were analyzed from a single experiment to determine the expected error in this approach. The goal of this analysis was to determine the void fraction, or the volume of bubble per unit volume water, under each set of conditions of wind

speed and rain rate, in order to determine the contribution of bubbles to the gas transfer velocity as in Ho *et al.* (2000). However, due to poor illumination and the high frequency of imaging, the images were typically underexposed, resulting in the impossibility of determining size spectra of the bubbles. Better backlighting or an optical setup similar to Asher and Farley (1995) or Ho *et al.* (2000) would greatly improve results of future experiments. We present our results below regarding the frequency of bubble formation to determine the effect of wind on the likelihood of bubble formation, but we are not able to quantitatively address the bubble-mediated portion of gas exchange in these experiments.

2.2.7 Wave slope

A He-Ne laser slope gauge, facing downward at the top of the tank, measured wave slope at a frequency of 1000 Hz. A receiver, placed below the tank, measured the distance of the refracted laser from its equilibrium position. The distance was calibrated to the slope by passing a clear plastic structure containing 12 sides of known angle to the horizontal below the slope gauge. Wave slope spectra were calculated using a 32-second Hanning window with 50% overlap. At least 100 min of data were analyzed from each experiment.

2.2.8 Gas tracer experiments

Approximately 20 pmol of sulfur hexafluoride (SF_6) dissolved in water were injected into the tank twice during each day of experiments. Following each injection, the wind generator was activated to create a nominal 10-m wind speed of 14 - 18 m s^{-1}, thus allowing the gas to mix throughout the tank (typically 1.5 - 2 hours mixing time). Samples from four locations in the tank were analyzed prior to each of these experiments to ascertain that the gas was well-mixed. During each experiment, 30-mL water samples were drawn from two depths (10 and 25 cm below the water surface) at two sampling stations located upwind and downwind of the rain module, using 50-mL glass syringes. Extreme care was taken to prevent bubbles from entering the tubing and syringes; if bubbles were detected, the sample was discarded. The suite

of samples was taken every 15 minutes over the course of each 2-hour experiment and samples were analyzed immediately after being drawn.

2.2.9 Gas evasion technique and calculations

SF_6 analysis

The principle and methodology of the SF_6 deliberate tracer evasion technique are described in detail by Wanninkhof *et al.* (1987). Water samples were analyzed for SF_6 concentrations using a headspace method (Wanninkhof *et al.*, 1987); a 20-mL headspace of ultra-high purity (UHP; 99.999%) nitrogen was added to each water sample, and the gas was allowed to equilibrate with the headspace through vigorous shaking on a wrist-action shaker for at least three minutes. The gas was then passed through a magnesium perchlorate ($Mg(ClO_4)_2$) drying column and injected onto a loop of known volume with UHP nitrogen as the carrier gas. The sample was then injected into an analytical column containing molecular sieve 5A. The mass of SF_6 was measured by an electron capture detector at 300^o C. SF_6 concentrations were normalized by peak area and calibrated to a standard concentration of 148.8 ppt (parts per trillion).

Calculations

The gas evasion technique allows determination of the air-water flux from knowledge of the waterside and airside concentrations of a tracer gas over a period of time; the following derivation is described in detail by Wanninkhof *et al.* (1987). Mathematically, the air-water flux of SF_6 is defined as the change of mass over time per unit area, where a positive flux is defined as gas evasion out of the water:

$$\mathrm{F} = -\frac{1}{A}\frac{dM_{\mathrm{SF_6}}}{dt} \tag{2.2.4}$$

Assuming that the gas is well-mixed in the tank, we can rewrite this as:

$$\mathrm{F} = -h\frac{d[\mathrm{SF_6}]}{dt} \tag{2.2.5}$$

where h is the depth of water in the tank, held constant throughout each experiment.

The flux can also be expressed as the product of the gas transfer velocity, k, and the difference in the measured waterside-SF_6 concentration and the saturation value, determined by the airside concentration and Ostwald solubility coefficient (α), calculated from the temperature dependence compiled by Wanninkhof (1992):

$$\mathrm{F} = k\left([\mathrm{SF}_{6,\mathrm{water}}] - \alpha[\mathrm{SF}_{6,\mathrm{air}}]\right) \tag{2.2.6}$$

Equating 2.2.5 and 2.2.6 and integrating over time $\Delta t = t_f - t_i$ to solve for the gas transfer velocity yields:

$$k = -h\frac{\Delta \ln\left([\mathrm{SF}_{6,\mathrm{water}}] - \alpha[\mathrm{SF}_{6,\mathrm{air}}]\right)}{\Delta t} \tag{2.2.7}$$

where $\Delta \ln\left([\mathrm{SF}_{6,\mathrm{water}}] - \alpha[\mathrm{SF}_{6,\mathrm{air}}]\right) = \ln\left([\mathrm{SF}_{6,\mathrm{water}}]_f - \alpha[\mathrm{SF}_{6,\mathrm{air}}]\right) - \ln\left([\mathrm{SF}_{6,\mathrm{water}}]_i - \alpha[\mathrm{SF}_{6,\mathrm{air}}]\right)$, and $[\mathrm{SF}_{6,\mathrm{water}}]_i$ is the waterside concentration of SF_6 at time $t = t_i$.

In the case of experiments with rain, the dilution due to rain must be accounted for (Ho *et al.*, 1997, 2000). In these experiments, the airside concentration of SF_6 never exceeded 35% of the waterside concentration. As the rain was in equilibrium with the air in the laboratory, we can determine the concentration of SF_6 in the raindrops; a calculation indicates that at the maximum air concentration, the gas transfer velocity would change by less than 0.1%. Thus, we approximate the rain as being free of SF_6, and the corrected gas transfer velocity is simply given by:

$$k = -h\frac{\Delta \ln\left([\mathrm{SF}_{6,\mathrm{water}}] - \alpha[\mathrm{SF}_{6,\mathrm{air}}]\right)}{\Delta t} - \frac{hP}{V} \tag{2.2.8}$$

where P is the volumetric rain rate and V is the volume of water in the tank.

The gas transfer velocity is known to be proportional to the ratio of the viscosity of the water to the diffusivity of the gas, a quantity defined as the Schmidt number, raised to a power less than 1. We normalize k to a Schmidt number of 600, equivalent to that of CO_2 in fresh water at 20^o C:

$$k_{600} = k_{\mathrm{SF}_6}\left(\frac{600}{\mathrm{Sc}_{\mathrm{SF}_6}}\right)^{-n} \tag{2.2.9}$$

Gas exchange models predict the value of the exponent, n, to range from $\frac{2}{3}$ in the case of a still surface without waves to $\frac{1}{2}$ in the case of a turbulent surface without breaking

waves (Deacon, 1977; Higbie, 1935). Empirical results have been found to corroborate the model predictions (Brumley and Jirka, 1988; Jähne *et al.*, 1984; Ledwell, 1984). In this experiment, we take $n = \frac{1}{2}$, except in the case of no wind or rain, where we take $n = \frac{2}{3}$.

The error in k_{600} was determined from the standard error in the slope of $\ln[\mathrm{SF}_{6,\mathrm{water}}]$ over time, assuming that the error in the water depth is negligible in comparison. This method of calculating the error accounts for the possibility that the water is not entirely well-mixed, as may be the case at low gas transfer velocities, as well as instrumental error.

2.3 Results

2.3.1 Wind

In the vicinity of the water surface (2 - 8 cm above the surface), wind speed profiles were found to be logarithmic; an example is shown in Figure 2.2. The slope of the curve and the y-intercept are therefore used to calculate the friction velocities and roughness lengths during each experiment.

2.3.2 Rain

Tank-averaged rain rates were determined for each experiment and are given in Table 2.2; the range of rain rates was grouped into low (8.1 - 12.1 mm h^{-1}), medium (14.1 - 18.4 mm h^{-1}) and high (24.1 - 27.1 mm h^{-1}). While it was not possible to achieve narrower ranges at each rain level due to technical issues with the hypodermic needles clogging, we use the actual rain rates in the parameterizations presented below, rather than the bin average.

In each experiment, the total kinetic energy flux was calculated based on the total impact velocity (horizontal plus vertical); this is considered rather than the vertical component only because KEF represents the total energy flux to the water surface. At the highest wind speed (21 m s^{-1}), the horizontal impact velocity was

13% of the total velocity, so neglecting this could have a significant impact on the kinetic energy flux calculation. This is discussed in more detail below.

2.3.3 Kinetic energy flux

The interactions of wind and rain on the kinetic energy flux (KEF) imparted to the water surface is illustrated in Figure 2.3. Here, the colored points represent the KEF due to rain (the three non-zero rain rates are easily distinguished as shades of light blue, yellow, and red). The solid line shows the KEF due to wind in the absence of rain, and the dashed line represents the KEF due to wind at the highest rain rate. While the KEF due to rain does not vary significantly with wind speed, it is of note that at each rain rate, the KEF due to rain decreases somewhat at 21 m s^{-1} winds. Additionally, as noted above, if we were to consider only the KEF imparted vertically, this effect would be significantly more pronounced, as the impact velocity of the raindrops decreases by 13% in this case. Therefore, the energy of the rain appears to decrease at higher wind speeds, and it appears that it is transferred to the wind, as the KEF due to wind increases at the highest rain rate. However, when the total KEF due to rain is considered, both of these effects are small in the conditions of the present study, so we will not parameterize this transfer of energy.

2.3.4 Turbulence and bubbles

Turbulent kinetic energy (TKE), related to the turbulence dissipation rate, ϵ, which has been found to scale with the gas transfer velocity to the fourth power (Kitaigorodskii and Donelan, 1984; Zappa *et al.*, 2009), was calculated from the power density spectra derived from flow measured by the ADV. An example of such a spectrum is shown in Figure 2.4. The -5/3 slope which is characteristic of turbulence is evident in this figure in the vertical flow component only; as this was common to many of the spectra, the TKE was calculated only from the vertical component by integrating below the power spectra within a band of frequencies common to all experiments ($10^{0.9}$ - 10^{1} Hz). The narrow band of frequencies was necessitated by differences in the location of the wave slope peak corresponding to waves rather than

turbulence in the tank. Values of TKE are presented below only from experiments which exhibited a -5/3 slope between these frequencies in the vertical component of the wave slope spectra. It is evident that both wind speed and rain rate increase the vertical TKE (see Figure 2.5). However, due to noise in many of the spectra at the intermediate rain rates, it was not possible to quantify the trend in TKE with rain rate, though it is evident that even at a wind speed of 21 m s^{-1}, a rain rate of 25 mm h^{-1} increases vertical TKE significantly. Noise in these data is mostly likely the result of a low sampling frequency, which was the highest possible for the ADV deployed. It is possible that water flow patterns due to raindrops varied on timescales similar to the sampling frequency, causing bias of the turbulence signal.

Regarding the second mechanism of gas exchange measured in this study, a typical bubble image from this study is shown in Figure 2.6. Due to poor exposure of the images, the quantification of bubbles in each experiment was limited to 1/10 the total number of images captured (3100), and sizing of the bubbles was not possible. In analyzing 7 different sets of 310 images from experiment 21, the standard deviation in the bubble frequency was estimated at 9.4%. The bubble formation frequencies measured in this experiment in the absence of wind are in reasonable agreement with those calculated from data measured by Ho *et al.* (2000); at a local rain rate of 66.4 mm h^{-1}, the total bubble formation frequency at the surface was approximately 0.23 according to data collected by Ho *et al.* (2000), while our data show formation frequencies of 0.16 and 0.28 at local rain rates of 48.8 and 82.9 mm h^{-1}, respectively. The frequency of bubble formation appeared to decrease with wind speed, in agreement with Medwin *et al.* (1990) as shown in Figure 2.7; however, due to a possibly significant error, these trends are not significant at the 95% confidence level. Indeed, while bubble formation increases with increasing rain rate in general, the difference is significant between rain rates of 10 and 16 mm h^{-1}, while in the case of some experiments, it appears that more bubbles form at a rain rate of 16 mm h^{-1} compared to 25 mm h^{-1}. Thus, while the bubble formation frequency may decrease slightly with wind speed, the rate of bubble formation increases with increasing rain rate.

2.3.5 Wave slope

The wave slope spectra, grouped by wind speed, are shown in Figure 2.8. In the absence of wind, the dominant wave slope due to rain appears at a frequency of 5 Hz. At low wind speeds (6.5 m s^{-1}), the frequency of this wave slope is governed by effects from the rain; in the absence of rain, the frequency of the dominant wave slope is approximately 6 Hz. Secondary and tertiary peak wave slopes occur, most likely attributable to the specific dynamics of this tank, at wind speeds of 10 m s^{-1} and above. At 14 m s^{-1} wind speeds, these additional peaks appear in all experiments, regardless of the presence of rain, which appears to dampen out these frequencies at lower wind speeds. Although the effects of rain are evident in the wave slope spectra at wind speeds lower than 14 m s^{-1} as the peak wave slopes occur at different frequencies for the rain and no-rain cases, the spectra are indistinguishable for our purposes at higher wind speeds. Thus, the effect of rain on wave slope appears to be negligible at wind speeds of 14 m s^{-1} and above.

2.3.6 Gas transfer velocities from SF_6

Figure 2.9 shows all gas transfer velocities measured in this experiment and normalized to a Schmidt number of 600, plotted as a function of the 10-m wind speed and rain rate. Gas transfer velocities ranged from 0.7 cm h^{-1} in the case of no wind or rain to 42.7 cm h^{-1} for $u_{10} = 20.9$ m s^{-1} and a tank-average rain rate of 27.1 mm h^{-1}. In the experiments with wind only, the maximum gas transfer velocity measured was 35.2 cm h^{-1}, and in the rain-only experiments, the maximum gas transfer velocity was 24.8 cm h^{-1}. Wind speeds, rain rates, kinetic energy fluxes, and corresponding gas transfer velocities are given in Table 2.2 for experiments with no rain and 23g hypodermic needle rain inserts and Table 2.3 for experiments with 20g hypodermic needle inserts.

2.4 Discussion

2.4.1 Kinetic energy flux

The kinetic energy flux is a useful measure to use in comparing the effects of wind and rain on air-water gas exchange as both of these drivers impart energy to the surface water, thus enhancing surface turbulence. Figure 2.3 shows the results of such a comparison. It is evident that the KEF due to wind increases significantly with increasing wind speed, whereas the KEF due to rain does not depend significantly on the wind speed. Of note in this figure is the intersection of the two plots, or the wind speeds and rain rates at which the kinetic energy flux of wind is equal to that of rain. The wind speeds at which $\mathrm{KEF_{wind}} = \mathrm{KEF_{rain}}$ for the three nominal rain rates in this study (10, 17, and 26 mm $\mathrm{h^{-1}}$) are 11.1, 13.0, and 14.7 m $\mathrm{s^{-1}}$, respectively. It has been proposed by Harrison *et al.* (in prep) that these points represent a regime shift: where the KEF due to wind is lower than that of rain, the combined effects of wind and rain on gas exchange are linearly additive, and when the KEF of wind exceeds that of rain, the effect of rain is significantly reduced. This provides a very good statistical description of the data (Harrison *et al.*, in prep). In the present experiment, however, these wind speeds do not correspond to where the effect of rain becomes negligible. Therefore, while the kinetic energy flux is most likely important in comparing the effects of wind and rain on the gas transfer velocity, a scaling parameter is necessary in comparing these quantities.

Here, we propose a mechanistic model based on the depth to which wind and rain effectively mix the water with respect to the gas tracer rather than an empirical model based on the kinetic energy fluxes. Mathematically, this is derived from Harrison's comparison of KEF due to wind and rain; we assume that the mixing depth of rain scales by $\mathrm{KEF_{rain}}$ (Green and Houk, 1979). We take the depth scale associated with wind to be the depth at which the turbulent kinetic energy has dissipated to a critical value. TKE dissipation has been found to scale with u_*^3/z (Dillon *et al.*, 1981; Soloviev *et al.*, 1988; Anis and Moum, 1995) where z represents depth in the upper 10 m of the ocean, yielding a characterisitic depth that scales with u_*^3 and thus with

KEF_{wind}. It has been shown in the laboratory that the relevant penetration depth of turbulence on the scales relating to gas exchange is approximately equal to the wavelength of wind-generated waves (Bliven *et al.*, 1984). In this case, the wavelengths of interest correspond to scales of capillary waves to small gravity waves, $\mathcal{O}(1) - \mathcal{O}(10)$ cm. This is comparable to the mixing depth as a function of rain measured by Green and Houk (1979).

Using the depth scale factors (KEF_{rain}, KEF_{wind}) and results from previous studies of the separate effects of wind (Wanninkhof, 1992; Ho *et al.*, 2006) and rain (Ho *et al.*, 1997, 2000) on gas exchange, we present a conceptual understanding of the combined effects of wind and rain below with the associated parameterization. We note that the scaling factor for the mixing depth of rain is based on the results of one study where the subject of interest was heat, not gas, transfer (Green and Houk, 1979). It is important to note, therefore, that the mechanism and parameterization proposed here are currently hypotheses only that are found to describe these data well, but future gas exchange studies should seek to better constrain the functionality of the mixing depth due to rain.

2.4.2 Gas transfer velocity

It is evident from Figure 2.9 that rain has a significant impact on the gas transfer velocity at low wind speeds, where a rain rate of 8.3 mm h^{-1} increases the gas transfer velocity by 5 cm h^{-1}, whereas at high wind speeds, the effect of rain is much reduced; a rain rate of 26 mm h^{-1} only increases the gas transfer velocity by 7 cm h^{-1} at a 10-m wind speed of 21 m s^{-1}. These results bear similarities to results from previous experiments at the ASIL (Ho *et al.*, 2007; Harrison *et al.*, in prep), as there appears to be a regime in which the effect of rain is significant over a range of wind speeds for a given rain rate; and a regime in which the effect of rain is significantly diminished. Following our proposed mechanism for understanding gas exchange in the presence of wind and rain, we compare a parameterization and sample calculation based on the assumption that the effects of wind and rain are

linearly additive to another parameterization derived from the mechanism proposed here.

Models

Wind and rain individually can enhance the gas transfer velocity significantly. However, given a fixed rain rate, the data from the present study as well as previous studies (Harrison *et al.*, in prep) indicate that the effect of rain on the gas transfer velocity diminishes with increasing wind speed (see Figure 2.9). It may be possible to explain this phenomenon by comparing the depth of dissipation of turbulent kinetic energy induced by the shear stress of wind to the mixing depth of the water due to rain.

For example, let us consider the case of a given rain rate. In the no-wind case, rain may be considered to mix the water with respect to the gas to a depth z_R. This mixing is caused by the vertical impact of raindrops impinging on the water surface. The mean depth of mixing over time would logically be a function of both the frequency and the size of the raindrops. As wind begins to blow, near-surface turbulence increases due to the shear force of the wind, and the gas transfer velocity correspondingly increases. At a low wind speed, the critical depth of dissipation of TKE due to wind, z_u, is significantly smaller than z_R. Between z_u and z_R (for $z_R > z_u$), rain continues to contribute to the mixing, thus enhancing gas exchange. However, as z_u approaches z_R, the difference between these mixing depths approaches zero, which is seen in our data as a diminishing effect of rain on the gas transfer velocity. This may be due to the difference in the mixing mechanisms of rain and wind; wind enhances turbulence at the surface significantly through a shear force. According to this proposed model, rainfall may increase the near-surface turbulence, but it does not mix the surface water any further with respect to the gas of interest, as the water is already well-mixed by wind from the surface to the critical depth z_u. If rain mixes the water to a depth greater than z_u, this causes the gas transfer velocity to increase corresponding to a function of the excess mixing of rain beyond that of the wind.

Empirically, in the absence of rain, the gas transfer velocity has been found to be a function of the square of the wind speed (Wanninkhof, 1992; Ho *et al.*, 2006):

$$k_{600} = a_{\mathrm{u}} u_{10}^2 \tag{2.4.1}$$

We take the units of a_{u} to be cm s^2 h^{-1} m^{-2}. Furthermore, in the absence of wind, k_{600} is a function of the KEF of rain; this can also be written in terms of the natural rain rate (Ho *et al.*, 1997, 2000). In this case, we use KEF in order to relate the gas transfer velocity to the mixing depth due to rain:

$$k_{600} = c_R \mathrm{KEF}_{\mathrm{rain}}^{\beta} \tag{2.4.2}$$

From results of Green and Houk (1979), we assume that the mixing depth with respect to rain scales with the kinetic energy flux:

$$z_R = \alpha_{\mathrm{R}} \mathrm{KEF}_{\mathrm{rain}} \tag{2.4.3}$$

where α_{R} has units of m^3 s J^{-1}. This allows us to recast Equation 2.4.2:

$$\begin{aligned} k_{600} &= a_{\mathrm{R}} \left(\mu z_R\right)^{\beta} \\ &= a_{\mathrm{R}} \left(\mu \alpha_{\mathrm{R}} \mathrm{KEF}_{\mathrm{rain}}\right)^{\beta} \end{aligned} \tag{2.4.4}$$

Note that $\mu = 1$ m^{-1} and the units of a_{R} are cm h^{-1}. We further assume that the critical depth for dissipation of TKE due to wind is proportional to $\mathrm{KEF}_{\mathrm{wind}}$, as above.

$$z_u = \alpha_{\mathrm{u}} \mathrm{KEF}_{\mathrm{wind}} \tag{2.4.5}$$

Here, α_{u} has units of m^3 s J^{-1}. Note that the 10-m wind speed is related to the friction velocity by the drag coefficient: $u_* = u_{10}\sqrt{\mathrm{C_D}}$. Because the drag coefficient is not constant with wind speed, u_{10} does not scale directly with the friction velocity.

The proportionality of the kinetic energy flux and critical depth of TKE dissipation is motivated by the fact that the transfer of energy from the wind to the water surface is manifested by an increase in turbulence at the water surface; the TKE dissipates near the surface, but this depth of critical dissipation is increased by a greater kinetic energy flux. It is also likely that the depth of critical dissipation is

influenced by the wind fetch, particularly in laboratory experiments where a single value of u_* and thus $\mathrm{KEF_{wind}}$ is determined for the tank. A greater fetch may increase the depth of critical TKE dissipation. This is discussed in more detail below when results from the large and small tanks are compared.

In combining wind and rain, it has been suggested that the effects would be linearly additive; this was proposed by Ho *et al.* (2007) and proved to be a good fit for the data in that study. In this case, the functionality of k_{600} would be:

$$k_{600} = a_{\mathrm{u}} u_{10}^2 + b\mathrm{KEF}_{\mathrm{rain}}^{\beta} \tag{2.4.6}$$

In this study, β and b were determined from the no-wind experiments to be 0.8378 and 60.1190 respectively; the data and this fit are shown in Figure 2.10. We determined a from the no-rain experiments to be 0.0894. The results of this parameterization compared to the measured gas transfer velocities in this experiment are shown in Figure 2.11. We note that, as expected, this parameterization captures gas transfer velocity data well in the cases of low wind; this regime is similar to that of WRX 1, in which it was found that the data could be described very well by a linear combination of wind speed and rain rate dependent functions (Ho *et al.*, 2007). However, at high k_{600}, corresponding to high wind speed experiments both in the presence and absence of rain, the linear parameterization over-predicts the gas transfer velocity by up to 16%. Thus, these data support the idea that the effects of wind and rain can be sufficiently approximated as linearly additive at low wind speeds, but this does not hold in the high wind speed regime.

As stated above, we are proposing that the effect of rain only depends on the extent to which rain mixes beyond the critical depth of wind TKE dissipation: substituting from above, this parameter should be given by $z_R - z_u$ in place of z_R in Equation 2.4.4:

$$\begin{aligned} k_{600} &= a_{\mathrm{u}} u_{10}^2 + a_{\mathrm{R}} \left[\mu \left(z_R - z_u\right)\right]^{\beta} && z_R \geq z_u \\ &= a_{\mathrm{u}} u_{10}^2 + b \left(\mathrm{KEF_{rain}} - c\mathrm{KEF_{wind}}\right)^{\beta} && \mathrm{KEF_{rain}} \geq c\mathrm{KEF_{wind}} \\ k_{600} &= a_{\mathrm{u}} u_{10}^2 && \mathrm{KEF_{rain}} < c\mathrm{KEF_{wind}} \end{aligned} \tag{2.4.7}$$

The comparison of this parameterization versus measured values of k_{600} is shown in Figure 2.12, where the value of c has been determined statistically to be 0.33.

It is clear that the model proposed here takes into consideration a great deal of the variability that is not captured in a model which assumes that the effects of wind and rain on the gas transfer velocity are linearly additive, particularly at high wind speeds (i.e. the highest gas transfer velocities). However, both the linearly additive parameterization and our proposed mixing parameterization account well for the observed gas transfer velocities up to approximately 30 cm h^{-1} in these experimental conditions. This is important to note as this was the extent of data presented by Ho *et al.* (2007); therefore, this proposed parameterization reconciles the "linearly additive" effects of wind and rain observed by Ho and colleagues as well as the data in the present study which demonstrate clearly that the combined effects of wind and rain on air-water gas exchange are not simply linearly additive.

In determining the parameters associated with the proposed model, it is important to note that a, b, and β can be determined with the no-wind and no-rain experiments. The value of c, however, has been determined from the combined wind and rain experiments, as it is not entirely well-known how the relevant depths related to wind and rain should be defined in the present context, and therefore the absolute values of z_u and z_R are not known. Furthermore, in applying this model to the results of the study described by Harrison *et al.* (in prep) (see Figure 2.13), we note that the value of c is greater than in the present study by a factor of 2. Not shown, this model can also be applied to the results of WRX 1 (Ho *et al.*, 2007), though because the non-linear term is insignificant in this experiment, the value of c cannot be further constrained. The value of c prescribed by the results of WRX 3, also conducted in the large tank, is applicable to the gas transfer velocity data from WRX 1 as well. From these results, we can assert that c is not a constant but is likely a function of the fetch, particularly in fetch-limited regions, as this coefficient represents the critical depth of dissipation of TKE due to wind and would therefore be expected to increase with increasing fetch. If it had been feasible to measure the friction velocity throughout the tank, it would be possible to determine the critical depth as a function of distance from the wind generator in the tank; however, the wind profile was determined only at a single fetch, resulting in a single value of $\mathrm{KEF_{wind}}$ for each value of u_{10}.

To relate the results from the present study to the field, it is necessary to determine the functional dependence of the coefficient c on the fetch. Although c can only be determined numerically in experiments with conditions of both wind and rain, we can derive an approximate relationship between these two parameters based on the relationship between the gas transfer velocity and fetch. Here we compare the results from WRX 3 and 8 at the ASIL as well as previous laboratory experiments in tanks of different fetch (see, for instance, Ocampo-Torres and Donelan, 1995, and references therein); the data are summarized in Table 2.4. From these results, it appears that k_{600} scales roughly with the fetch to the power of 0.25; thus, c should scale approximately with fetch$^{0.43}$. This is in good agreement with the values of c determined from experiments in the small and large tanks at the ASIL. However, it is important to note that this dependence of k_{600} and c on fetch is based on experiments with fetch ranging from 2 to 40 m. For a larger fetch, this relationship is not well known. Therefore, in applying these results to the ocean, where the fetch may be unlimited, it is possible that c approaches an upper limit, though it is not yet known what that limit would be.

Relating these data to the field, and specifically to oceanic regions where high speeds are common such as the Southern Ocean, this mechanistic model predicts that the effect of rain on the gas transfer velocity would be less significant than what would be predicted by a model assuming the effects of wind and rain on gas exchange are linearly additive. With regard to the gas flux, it has been found that rain can significantly affect the ΔpCO_2, thus enhancing or dampening the magnitude and determining the direction of the flux (Turk *et al.*, 2010), though the gas transfer velocity may not change significantly. In certain aquatic environments including coastal wetlands regions, such as the Everglades, the nonlinear effects of wind and rain on the gas transfer velocity may play an important role in constraining the gas transfer velocity. By way of example, we take the case of a typical low wind speed measured in June 1997 by Lindberg and Zhang (2000) and high wind speed measured in the aforementioned study in March 1998, and common rain rates during these seasons. The friction velocities were determined from the COARE algorithm Fairall *et al.* (2003) based on typical air and water temperatures and relative humidity data

for these months. These values are given in Table 2.5. Using the parameterization proposed by Ho *et al.* (2006) for the wind speed dependence of gas exchange and a relationship between KEF due to rain and gas transfer velocity based on that derived by Ho *et al.* (1997), we apply the non-linear correction to the gas transfer velocity proposed here to derive a conservative estimate of the effect of rain on air-sea gas exchange:

$$k_{600} = 0.266u_{10}^2 + 39.36\left(\mathrm{KEF_{rain}} - 0.33\mathrm{KEF_{wind}}\right)^{0.578} \tag{2.4.8}$$

We use the relationship between $\mathrm{KEF_{rain}}$ and the natural rain rate, $\mathrm{R_n}$, derived by Ho *et al.* (1997), assuming a raindrop distribution given by Marshall and Palmer (1948) and terminal velocities predicted by Gunn and Kinzer (1949):

$$\mathrm{KEF_{rain}} = 3.43 \times 10^{-3}\mathrm{R_n^{1.17}} \tag{2.4.9}$$

Here, KEF is in units of J $\mathrm{m^{-2}}$ $\mathrm{s^{-1}}$ and $\mathrm{R_n}$ is in units of mm $\mathrm{h^{-1}}$.

In Table 2.5, we compare the results for calculated gas transfer velocity assuming (1) no effect from rain, (2) the effects of wind and rain are linearly additive, and (3) the effects of wind and rain scale according to Equation 2.4.8. We can see here that rain plays a significant role in gas exchange in these regimes, and while the effects of wind and rain can be approximated as linear in low wind speed, high rain rate regimes, we note a 1% decrease in k_{600} under higher wind speed, lower rain rate conditions typical of March weather. While this difference may be small in magnitude, it may be significant in flux calculations in areas of large air-water disequilibria of gas concentrations. Figure 2.14 shows a comparison of the gas transfer velocity that would be predicted assuming a linearly additive model of the effects of wind and rain (dashed lines) vs. gas transfer velocities predicted by the model proposed here (solid lines) at different wind speeds and rain rates, using the coefficients presented in 2.4.8. This figure shows the regimes in which the effects of wind and rain can be approximated as linearly additive, as well as the approximate wind speeds at which the effect of rain becomes negligible.

With respect to the global oceanic CO_2 flux, Figure 2.15 illustrates the influence of rain on the gas transfer velocity in the tropics predicted by the model proposed here. The wind speed data are derived from National Center for Environ-

mental Prediction (NCEP/NCAR) reanalyzed wind data (daily average); the rain rates are 3-day averaged rain rates for the middle day from the Tropical Rainfall Measuring Mission (TRMM); these data are accessible from the Asia-Pacific Data-Research Center datasets (APDRC: http://apdrc.soest.hawaii.edu/data/data.php). The CO_2 partial pressure gradient data is from Takahashi *et al.* (2009). This figure shows the average annual influence of rain for the year 2000. While the net effect of rain in the tropics is small ($\approx 0.9\%$), Figure 2.15 shows that locally, the gas transfer velocity and flux may be enhanced by up to 16%, particularly in the Western Equatorial Pacific, where wind speeds are typically low and rain rates are often high. Compared to an estimated error of 50% on the global net CO_2 flux predicted by Takahashi *et al.* (2009), the effect of rain on the gas flux via the gas transfer velocity may not be significant. However, it is also known that rain affects the CO_2 concentration gradient across the air-sea interface through formation of a fresh-water lens and wet deposition of CO_2 from the atmosphere, and that this effect may be significant (Komori *et al.*, 2007; Turk *et al.*, 2010). Specifically, rain transports CO_2 from the atmosphere to the oceans, as raindrops are in equilibrium with the atmosphere, and this may change the direction of the gas flux at the interface. In this study, we focus only on the effects of wind and rain on the gas transfer velocity, so these effects are not taken into account here. It is therefore possible that rain has a more pronounced effect on the local oceanic CO_2 flux than shown in this figure.

2.4.3 Turbulence

Turbulence is the dominant mechanism driving gas exchange due to both wind and rain. While the model suggested and discussed above does not explicitly take turbulence into account, we are proposing that the critical depth of wind mixing can be defined by the dissipation profile of turbulent kinetic energy. We did not use the TKE data collected here to quantify k_{600} because we were not able to measure TKE profiles, and we did not gather enough data to quantitatively investigate the dependence of the gas transfer velocity on near-surface TKE at a given depth in the water column. Additionally, because it was necessary to integrate the wave slope

spectra over a narrow band of frequencies as discussed above, the error in the TKE values may be significant. For that reason, we use the quantitative data only to compare the turbulence in different conditions of wind and rain qualitatively.

Interestingly, we are able to surmise that the gas transfer velocity is not directly proportional to the TKE at a fixed depth (in this case, 10 cm) under combined wind and rain conditions. This is evidenced by Figure 2.5, where it appears that the effects of wind and rain on TKE are linearly additive at 10 cm below the water surface, or at least that rain has a significant impact on the TKE even at high wind speed (21 m s^{-1}). We suggest that in conditions where the mixing depth of rain is greater than that of wind, wind enhances TKE from the surface to z_u, and the effect of rain on the gas transfer velocity only depends on the additional TKE enhancement below z_u. It would be instructive to perform a more detailed analysis of TKE or turbulent energy dissipation in gas exchange experiments under combined conditions of wind and rain, such as conducted by Zappa *et al.* (2009).

2.4.4 Wave slope

The wave slope spectra, shown in Figure 2.8, show results of the physical interaction between wind and rain on the wave field at the air-water interface. However, this is not a robust parameter for calculating the gas transfer velocity, at least for the frequency at which the wave slope was measured in this study. This is evidenced by the fact that the spectra from experiments with and without rain are indistinguishable at a 10-m wind speed of 14 m s^{-1} and higher. The corresponding gas transfer velocity data suggest that the same rain rates can have a significant effect on k_{600} at a wind speed of 14 m s^{-1}.

Previous studies have shown that the mean square slope of the wave field scales well with the gas transfer velocity when an appropriate range of wavenumbers is considered (Frew *et al.*, 2004). However, as the wave field was not adequately characterized in this experiment (neither wavenumber nor wave height were measured), we were not able to carry out this analysis.

2.5 Summary and Conclusions

Results from gas exchange experiments under varying conditions of wind speed and rain rate illustrate that the combined effects of these two driving forces of air-water water gas exchange are not linearly additive, as hypothesized and found in previous studies (Ho *et al.*, 2007; Harrison *et al.*, in prep). If we assume that the relevant depths of mixing due to rain and TKE dissipation due to wind scale with $\mathrm{KEF}_{\mathrm{rain}}$ and $\mathrm{KEF}_{\mathrm{wind}}$, respectively, then we have shown that this effect is particularly notable in regimes where the TKE due to wind has dissipated significantly only below the depth of water that is mixed by rain. Future experiments should further investigate these relationships relating to the relevant depth scales. We propose a parameterization to explain this data: $k_{600} = au_{10}^2 + b\left(R_n^{1.17} - c\rho_a u_*^3\right)^{\beta}$, where u_{10} is the wind speed at 10 m, R_n is the natural rain rate, ρ_a is the density of air, and u_* is the friction velocity. In fetch-limited regions, it is likely that c scales approximately with the square root of the fetch. In application to field studies, each of these parameters is routinely measured. The data in this and previous studies suggest that in the presence of wind and rain, the effect of rain on turbulence affecting gas exchange is negligible between the surface and z_u. However, in the case that the mixing depth of rain is deeper, $z_R > z_u$, the effect of this excess mixing on the gas transfer velocity is added to the effect of turbulence due to wind.

Turbulence data suggests that TKE due to wind and rain at a fixed depth may be linearly additive in the experimental regime considered here, though further studies are require to determine this quantitatively. Wave slope spectra, while descriptive of physical interactions between rain and wind waves, do not yield insight into the effects of wind and rain on gas exchange, as the effects of rain on wave slope vanish from the spectra before the effect of rain on gas exchange diminishes significantly.

The results presented here are applicable to gas exchange experiments in freshwater systems. However, rain falling on salty water causes a density gradient to evolve. Although previous gas exchange studies in saltwater (Ho *et al.*, 2004) have demonstrated that the gas transfer velocity under rainy conditions is equal to what

is found in freshwater experimental setups, it may be that the combination of wind and rain behave differently. Future studies should examine the critical depths of wind and rain with respect to dissipation of TKE and mixing, respectively, in saltwater to adequately parameterize the gas transfer velocity in terms of these two variables.

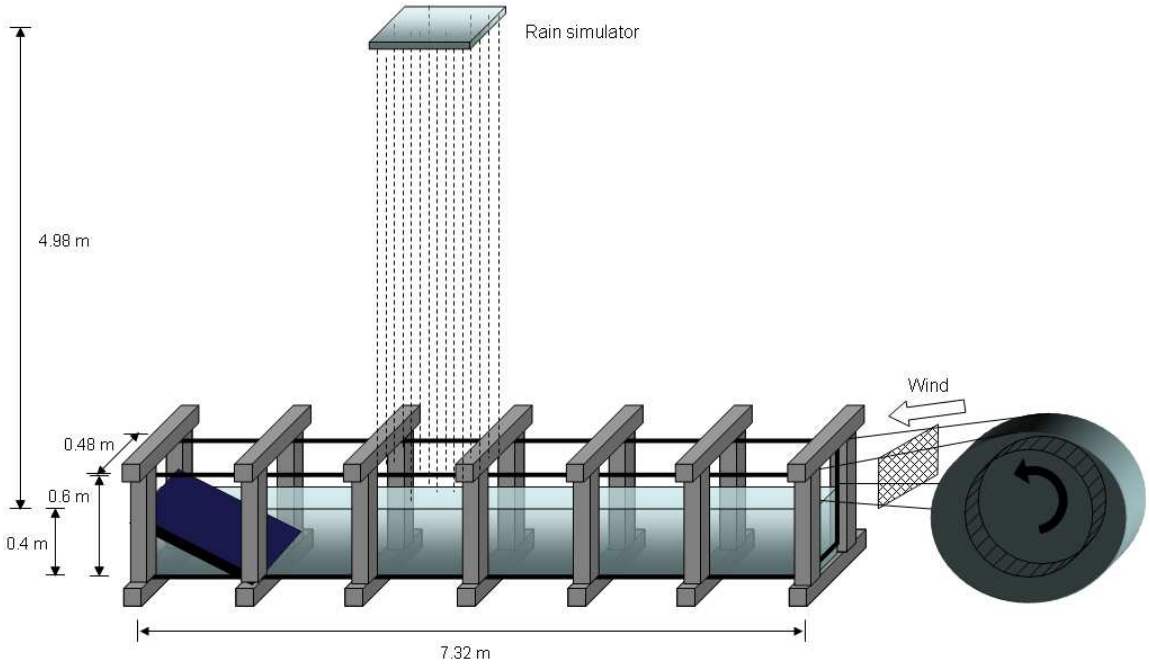

Figure 2.1: Small wind-wave-current tank used for gas exchange experiments in WRX 8; diagram created by Emily Harrison and Marc Buckley

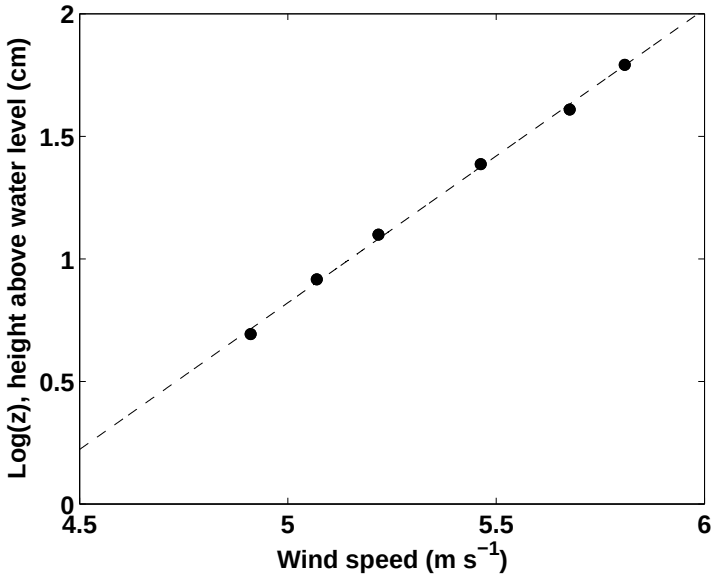

Figure 2.2: Example of wind speeds above the water surface and interpolated logarithmic wind speed profile from WRX 8, experiment 32

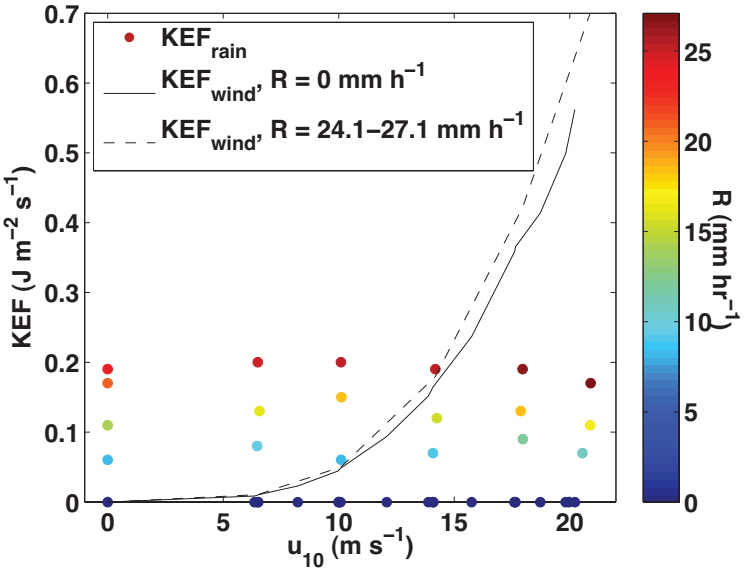

Figure 2.3: Kinetic energy flux of rain and wind impacting the water surface

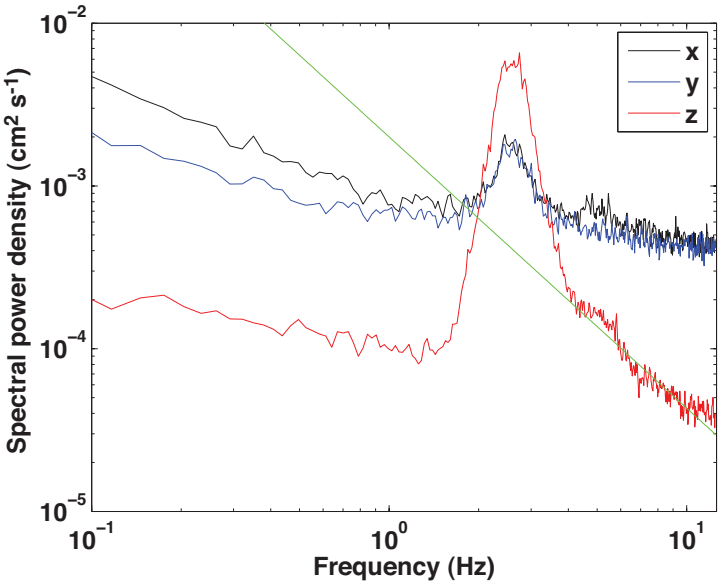

Figure 2.4: Turbulence density spectra in three dimensions, experiment 13. Green line shows -5/3 slope

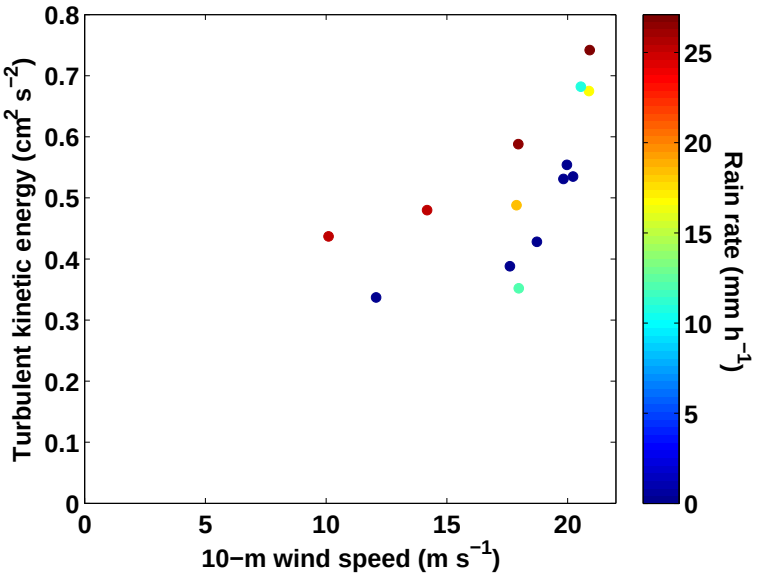

Figure 2.5: Turbulent kinetic energy as a function of wind speed and rain rate

Figure 2.6: Sample image of bubble forming at air-water interface

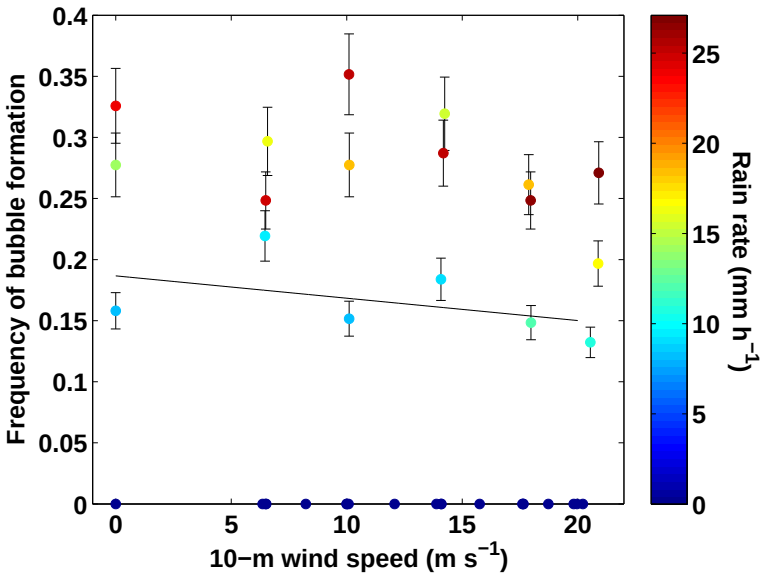

Figure 2.7: Frequency of bubble formation as a function of rain rate and wind speed. Solid line shows trend in frequency at lowest rain rate (8.1 - 12.1 mm h^{-1}), though slope is not significantly different from 0 at 95% confidence level

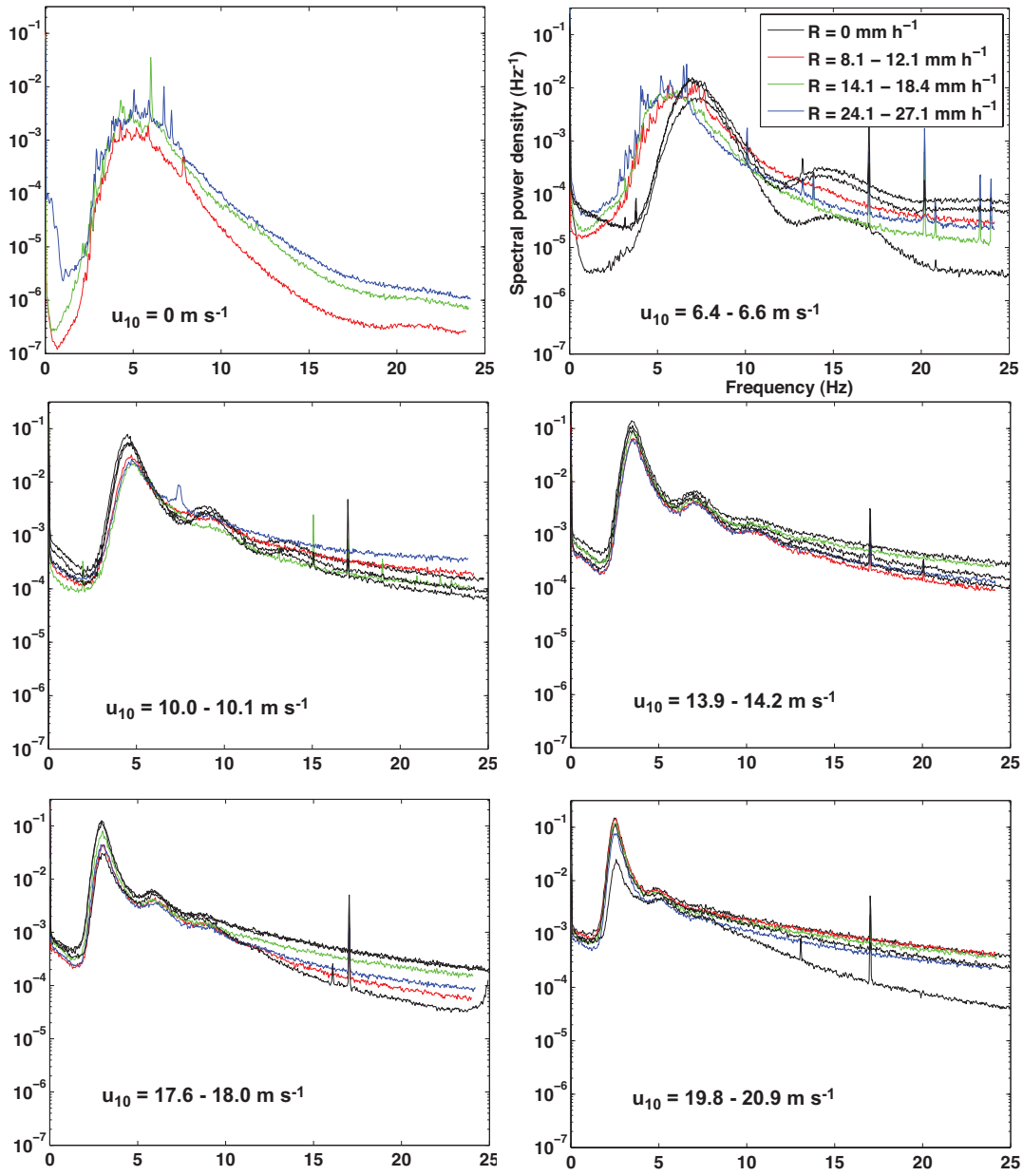

Figure 2.8: Wave slope spectra grouped by wind speed; no rain (black), low rain rate (red), medium rain rate (green), high rain rate (blue). At wind speeds below 14 m s^{-1}, the spectral power densities for rain and no-rain cases show distinct frequencies of peak wave slopes. The spectra are indistinguishable for our purposes at wind speeds of 14 m s^{-1} and above, signifying the reduced effects of rain on the wave slope at this wind speed

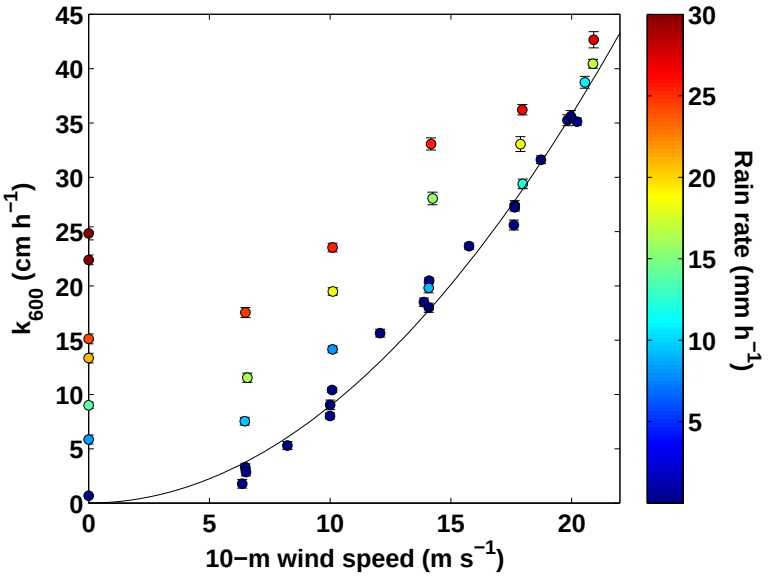

Figure 2.9: Gas transfer velocities measured in WRX 8; solid line shows parameterization for k_{600} as a quadratic function of the 10-m wind speed

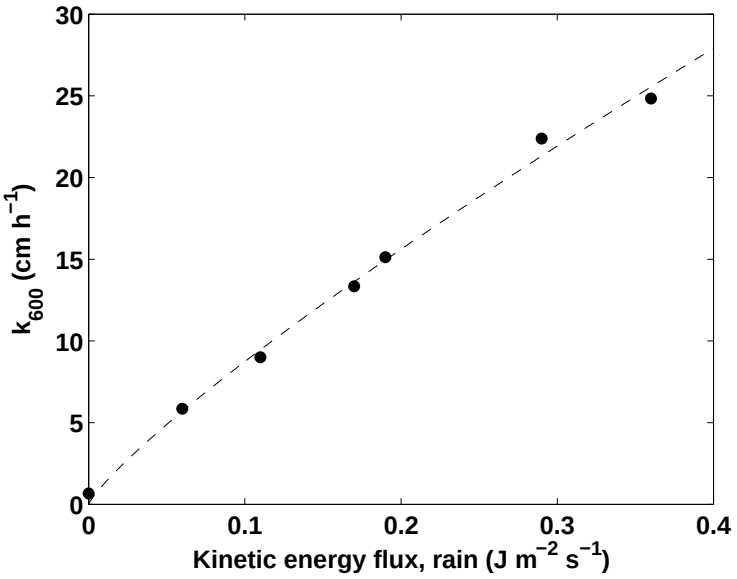

Figure 2.10: Gas transfer velocity from no-wind experiments parameterized as a function of the the kinetic energy flux of rain

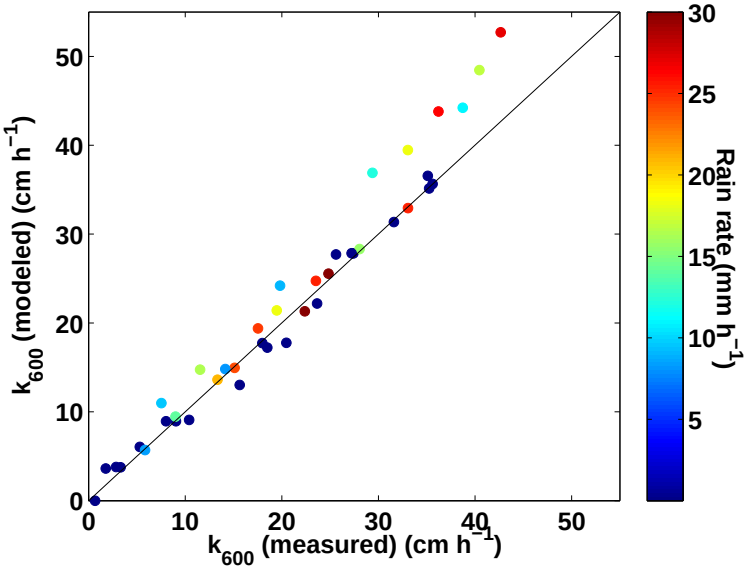

Figure 2.11: Comparison of k_{600} measured in all WRX 8 experiments to gas transfer velocities derived from a parameterization of the functional form in Equation 2.4.6

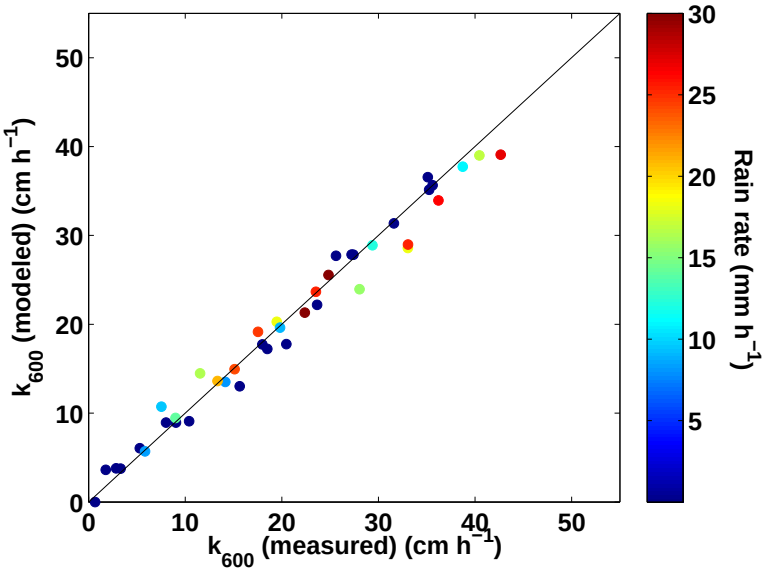

Figure 2.12: Comparison of k_{600} measured in all WRX 8 experiments to gas transfer velocities derived from a parameterization of the functional form in Equation 2.4.7

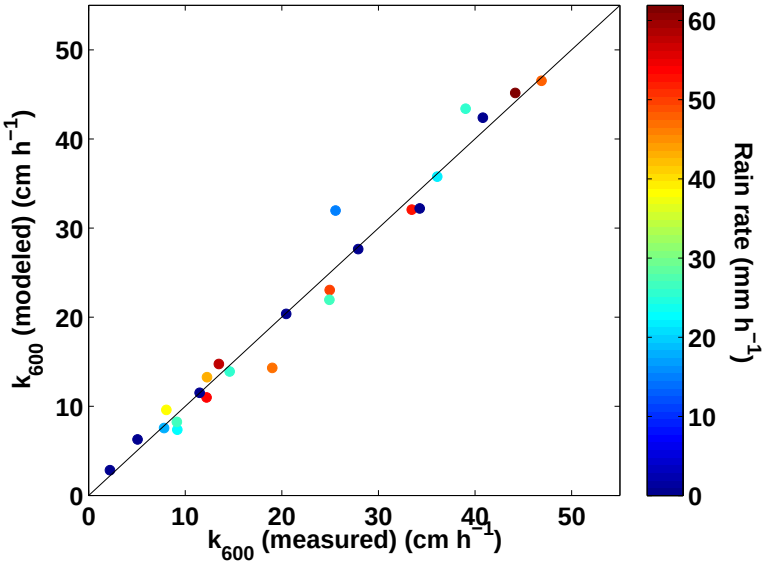

Figure 2.13: Comparison of k_{600} measured in all WRX 3 (Harrison *et al.*, in prep) experiments to gas transfer velocities derived from a parameterization of the functional form in Equation 2.4.7

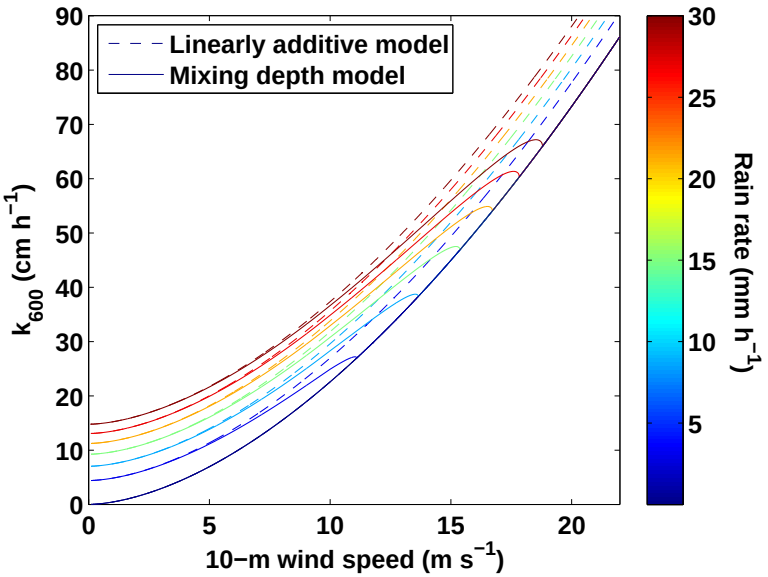

Figure 2.14: Comparison of gas transfer velocities predicted by linearly additive model (Equation 2.4.6; dashed lines) and mixing depth model proposed here (solid lines; Equation 2.4.7)

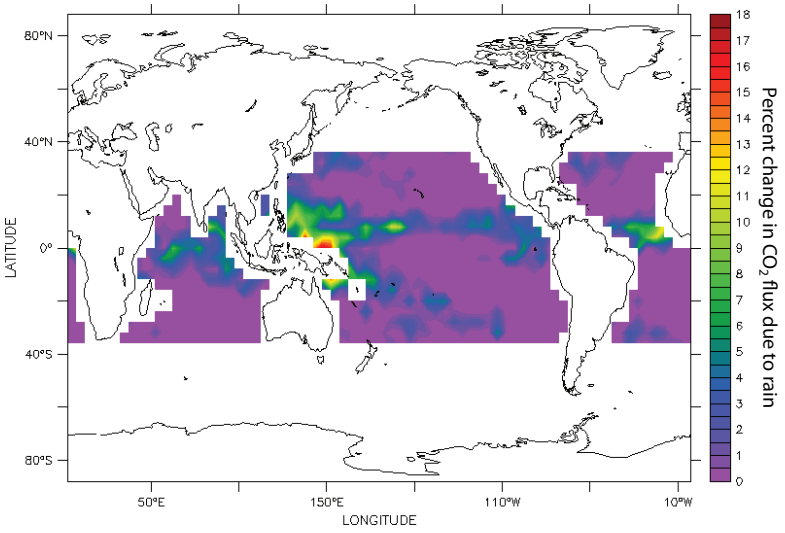

Figure 2.15: Net annual effect of rain on the CO_2 gas flux in the tropics, expressed as a percentage of total gas flux. Here, only the effect of rain on the gas transfer velocity is taken into account; the dependence of the interfacial CO_2 gradient is neglected

	Tank	Rain coverage (% tank surface area)	Wind speeds (m s^{-1})	Rain rates (mm h^{-1})	No. exps
WRX 1	Large	4%	0 - 13	0 - 26	12
WRX 2	Large	50%	N/A	N/A	N/A
WRX 3	Large	50%	0 - 19	0 - 62	27
WRX 4	Large	50%	3.5 - 16	0 - 49	15
WRX 5	Small	17%	0 - 24	0 - 17	12
WRX 6	Large	50%	3.5 - 16	0 - 48	12
WRX 7	Small	17%	N/A	N/A	N/A
WRX 8	Small	17%	0 - 21	0 - 46	44

	Comments
WRX 1	Pilot experiments in large tank; results indicated that effects of wind and rain on gas exchange are linearly additive
WRX 2	Test experiments with new rain module setup
WRX 3	At extended wind speeds and rain rates, results showed that effect of rain becomes negligible when $KEF_{wind} = KEF_{rain}$
WRX 4	Investigated anomalies in WRX 3 results; data showed lower gas transfer velocities at wind and rain conditions comparable to WRX 3
WRX 5	Pilot experiments in small tank
WRX 6	Investigated possible presence of surfactants and difference between WRX 3 and 4
WRX 7	Bubbling introduced by recirculating pumps affected gas evasion rates
WRX 8	Data presented here

Table 2.1: Summary of Wind-Rain eXperiments (WRX) conducted at the Air-Sea Interaction Laboratory, 2005 - 2010

Exp	u_{10} (m s^{-1})	u_* (m s^{-1})	Rain rate (mm h^{-1})	KEF$_{\text{wind}}$ (J m^{-2} s^{-1})	KEF$_{\text{rain}}$ (J m^{-2} s^{-1})	k_{600} (cm h^{-1})
2	0.0	0.00	0.0	0.000	0.000	0.7 ± 0.1
3	6.4	0.19	0.0	0.008	0.000	1.8 ± 0.4
4	10.0	0.34	0.0	0.046	0.000	9.0 ± 0.4
5	13.9	0.50	0.0	0.152	0.000	18.5 ± 0.4
6	14.1	0.52	0.0	0.165	0.000	18.0 ± 0.4
7	6.5	0.20	0.0	0.010	0.000	3.3 ± 0.3
8	10.0	0.33	0.0	0.045	0.000	8.0 ± 0.3
9	8.2	0.27	0.0	0.023	0.000	5.3 ± 0.4
11	19.8	0.75	0.0	0.499	0.000	35.3 ± 0.5
13	20.9	0.83	16.8	0.695	0.106	40.5 ± 0.4
14	0.0	0.00	8.3	0.000	0.064	5.9 ± 0.4
15	17.6	0.67	0.0	0.358	0.000	25.6 ± 0.5
16	20.2	0.78	0.0	0.562	0.000	35.1 ± 0.3
17	20.9	0.84	27.1	0.703	0.171	42.7 ± 0.7
18	0.0	0.00	14.1	0.000	0.109	9.0 ± 0.3
19	20.5	0.81	10.9	0.629	0.069	38.7 ± 0.5
20	17.6	0.67	0.0	0.362	0.000	27.4 ± 0.4
21	0.0	0.00	24.1	0.000	0.187	15.1 ± 0.5
22	17.9	0.70	18.3	0.410	0.135	33.1 ± 0.7
23	6.5	0.20	9.5	0.010	0.077	7.5 ± 0.4
24	6.5	0.20	0.0	0.010	0.000	2.9 ± 0.3
25	18.0	0.71	26.4	0.422	0.195	36.2 ± 0.5
26	6.6	0.21	16.5	0.011	0.134	11.5 ± 0.4
27	18.0	0.70	12.1	0.419	0.089	29.4 ± 0.4
28	14.1	0.52	0.0	0.165	0.000	20.5 ± 0.3
29	10.1	0.35	25.4	0.050	0.201	23.5 ± 0.4
30	14.2	0.53	15.6	0.180	0.117	28.1 ± 0.6
31	10.1	0.35	8.1	0.049	0.064	14.2 ± 0.3
32	10.1	0.34	0.0	0.048	0.000	10.4 ± 0.2
33	14.2	0.53	25.4	0.179	0.191	33.1 ± 0.6
34	10.1	0.35	18.4	0.050	0.145	19.5 ± 0.3
35	14.1	0.52	9.1	0.165	0.068	19.8 ± 0.5
36	18.7	0.70	0.0	0.414	0.000	31.6 ± 0.4
37	6.5	0.21	24.7	0.010	0.201	17.5 ± 0.5
38	15.8	0.58	0.0	0.237	0.000	23.7 ± 0.3
39	12.1	0.43	0.0	0.094	0.000	15.6 ± 0.4
40	20.0	0.76	0.0	0.522	0.000	35.6 ± 0.5
41	17.7	0.67	0.0	0.365	0.000	27.2 ± 0.3
42	0.0	0.00	45.6	0.000	0.364	24.8 ± 0.6
43	0.0	0.00	36.8	0.000	0.293	22.4 ± 0.4
44	0.0	0.00	20.8	0.000	0.166	13.3 ± 0.4

Table 2.2: Results of gas exchange experiments using 23g hypodermic needles in rain modules

Exp	u_{10} (m s^{-1})	u_* (m s^{-1})	Rain rate (mm h^{-1})	KEF$_{\text{wind}}$ (J m^{-2} s^{-1})	KEF$_{\text{rain}}$ (J m^{-2} s^{-1})	k_{600} (cm h^{-1})
42	0.0	0.00	45.6	0.000	0.364	24.8 ± 0.6
43	0.0	0.00	36.8	0.000	0.293	22.4 ± 0.4
44	0.0	0.00	20.8	0.000	0.166	13.3 ± 0.4

Table 2.3: Results of gas exchange experiments using 20g hypodermic needles in rain modules

Short fetch (m)	Long fetch (m)	Increase in k_{600} (%)	
16	32	20	Ocampo-Torres and Donelan (1994, 1995)
8	18	30	Merlivat and Memery (1983), Broecker *et al.* (1978)
2	8	20 - 40	Jähne *et al.* (1989)
7.3	38	58	This study, Harrison *et al.* (in prep)

Table 2.4: Comparison of results from gas transfer velocity experiments in the laboratory to determine the dependence of k_{600} on fetch; k_{600} is larger at comparable wind speeds in tanks with larger fetch by the percentage indicated here

u_{10} (m s^{-1})	u_* (m s^{-1})	Rain rate (mm h^{-1})	k_{600} (cm h^{-1})		
			(a)	(b)	(c)
1.4	0.012	10.0	0.5	7.5	7.5
3.9	0.093	3.0	4.0	7.2	7.1

Table 2.5: Application to the field: Typical conditions in the Everglades and associated gas transfer velocities assuming (a) no effect of rain, (b) linearly additive effects of wind and rain, (c) relationship presented in Equation 2.4.8

Chapter 3

Gas Exchange in a Ridge and Slough Region in the Everglades

3.1 Introduction

Gas exchange is a crucial process to quantify in order to constrain both global and regional carbon budgets. Biological studies that aim to describe various parameters of ecosystem dynamics, such as respiration, gross primary production, and net primary production must take into account the air-water flux of biologically important gases, including CO_2 or O_2, as this process can be of the same order of magnitude as rates of biological processes (Odum, 1956; Caffrey, 2004). In studying local carbon budgets and air-water fluxes of CO_2, lakes and wetlands are of particular interest as study sites such as these are typically highly productive regions that can be large sources of biologically and climatically important gases to the atmosphere (see, for instance, Cole *et al.*, 2007, and references therein).

The Everglades, one of the largest wetland systems in North America, is of interest in biological studies of the aforementioned nature because the ecosystem dynamics of this region have changed dramatically over time (Science Coordination Team, 2003). Further, efforts have begun to restore the water flow of the Everglades to original conditions, by deconstructing significant structures that have been erected across this area over the past century. Altering the water flow will have implications for the many diverse biological species in this region; as such, it is important to

understand the current state of the ecosystem before alterations to the landscape are made.

Hagerthey *et al.* (2010) conducted such a study; the authors monitored dissolved oxygen concentrations over a period of time in several different regions of the Everglades, including oligotrophic and eutrophic environments. This allowed calculation of rates of net primary production and respiration. By inferring gas transfer velocities, the authors calculated rates of gross primary production at each study site and thus compared the ecosystem characteristics with the corresponding metabolic rates. It is important to assert that the rates of gas exchange in this study were not measured directly, but rather were inferred from measured wind speeds; this is commonly done in studies of this nature, as multiple parameterizations for the gas transfer velocity have been developed over time (e.g. Wanninkhof, 1992; Cole and Caraco, 1998). These parameterizations are typically polynomial, piecewise linear, or power law fits of the gas transfer velocity to wind speed, based on data points from wind tunnels, lakes, estuaries, rivers, or oceans. Selecting an appropriate parameterization is important, but not always straightforward (Raymond and Cole, 2001). Furthermore, predicting the gas transfer velocity based on wind speed requires knowledge of the wind speed profile above the water, which may be approximately logarithmic over the open ocean (e.g. Fairall *et al.*, 2003) but can be more complicated in wetland regions where dense vegetation affects the wind speed near the surface (e.g. Finnigan, 2000).

In the study conducted by Hagerthey *et al.* (2010), the gas transfer velocity was parameterized according to Cole and Caraco (1998):

$$k_{600} = 2.07 + 0.215 \cdot u_{10}^{1.7}$$

This relationship (hereafter denoted as CC98) is derived from studies in an oligotrophic lake characterized by low wind speeds (average wind speed 1.39 $\pm$ 0.06 m s^{-1}), not unlike the range of wind speeds typically measured in the Everglades (1.4 $\pm$ 0.9 m s^{-1} during low wind speed periods; 3.9 $\pm$ 2.3 m s^{-1} during high wind speed periods (Lindberg and Zhang, 2000)). At wind speeds higher than 3 m s^{-1}, the driving mechanism of gas exchange is typically wind; however, at lower wind speeds, gas

exchange is weakly dependent on wind speed, and buoyancy fluxes may be the driving mechanism (Livingstone and Imboden, 1993; Soloviev and Schlüssel, 1994; Clark *et al.*, 1995). Water flow in the Everglades is typically low, similar to lakes, and unlike estuaries where tidal velocities and bottom topography can play important roles in enhancing water surface turbulence and therefore gas exchange (Raymond and Cole, 2001). Of note, however, is that the Everglades is comprised of a wide variety of habitats, including both eutrophic and oligotrophic ecosystems (indeed, Hagerthey and colleagues conducted experiments in a range of environments), whereas CC98 is based on data points from an oligotrophic environment. Hagerthey *et al.* (2010) assumed that wind speeds at the study sites were equal to those measured at a nearby meteorological station except in regions of dense vegetation, where the wind speed was taken to be zero, reflecting the impact of vegetation on the wind speed profile.

Biology and productivity can play an important role in air-water gas flux in many respects: photosynthesis and respiration change the waterside concentration of biologically important gases, including CO_2 and O_2, thus influencing the air-water gradient and both the magnitude and direction of the flux. Biology also plays a role in mediating the gas transfer velocity through the production of surface-active materials. Highly productive ecosystems are often marked by high levels of surfactants, which reduce the gas transfer velocity mainly by reducing turbulence at the surface (Frew *et al.*, 2004). Vegetation may impact air-water gas exchange by floating at the water surface, thus reducing turbulence near the water surface as well as imposing a physical barrier to gas exchange. Flora or other physical barriers that extend above the water surface, such as sawgrass (*Cladium jamaicense*), commonly found in the Everglades, may impact the wind profile above the water surface, thus reducing turbulence at the air-water interface and consequently reducing the gas transfer velocity.

In this study, we present findings from a series of gas transfer velocity experiments performed in two limnocorrals in a eutrophic area of the Everglades. The study site was located in a region where the ridge and slough system is highly degraded and periphyton is present in abundance. The limnocorrals were erected not far from the bordering sawgrass. The first goal of the experiment was to determine the effect of the sawgrass on the wind profile and hence on gas exchange in the lim-

nocorrals. The gas transfer velocities measured here were then compared to CC98 to assess the accuracy of the latter in this particular environment. In the discussion, we include a comparison to a second parameterization proposed by Wanninkhof (1992) and MacIntyre *et al.* (1995), based on several gas exchange studies in lakes, for comparison (hereafter, W92):

$$k_{600} = 0.45 \cdot u_{10}^{1.64}$$

In the sections below, we present a detailed description of the technique for measuring gas exchange in the Everglades using two limnocorrals. We made use of this method to determine the gas transfer velocity in this environment under naturally occurring wind speeds. We compare wind speeds measured below the sawgrass height to those measured at a nearby meteorological station at 10 m, allowing us to examine the impact of the sawgrass on the wind speed profile. Section 3 describes the results, followed by a short discussion in Section 4 and summarized by our conclusions in Section 5.

3.2 Methods

3.2.1 Everglades research site

Two limnocorrals and a tripod were erected for the present experiment in the Florida Everglades located at 25.85128^o N, 80.62158^o W. While this site is located in a part of the ridge and slough landscape typical of the Everglades, it is between water conservation areas (WCA) 3A and 3B, where the ridge and slough features are now highly degraded. Many types of periphyton, including floating mats of floral species, are present in abundance. The study site was located in an area of water surrounded by sawgrass that averages 1 - 2 m above the water surface in this region. While much of the periphyton is present in the water as floral mats floating at the water surface, a significant portion of the surface remains unobstructed.

To facilitate this experiment, a platform was erected adjacent to the two limnocorrals, allowing for personnel, equipment, and instrument storage, shown in

Figure 3.1. Additional instruments were mounted on a tripod, which extended 3 m above the water surface and was erected several meters north of the platform and approximately 2 m from the bordering sawgrass. The platform directly bordered both of the limnocorrals, providing a barrier to prevent the wind from moving the corrals. The platform was 2 m long and 30 cm wide and was elevated approximately 0.5 m above the water surface; it is unlikely that it would have impacted the wind field significantly in any direction. The limnocorrals were plastic and 1.5 m in diameter; the top of each was inflated to provide a barrier to water transport into or out of the corral. The inflated ring extended approximately 10 cm above the mean water surface. On Day 1, it became clear that the inflatable barrier was impacting the wind-induced turbulence, as ripples at the water surface outside of the corral were evident while the water inside the corral remained calm. The inflatable barrier was subsequently deflated to extend approximately 5 cm above the water surface, and remained so for experiments on Days 2 - 4. We present results from Day 1 below but not for quantitative comparison with Days 2 - 4. The first limnocorral (LC1) was free of any macrofloral species; several species of macrophytes, including floating mats, were added to LC2 in an effort to determine the effect of periphyton on gas exchange. It is important to note, however, that the periphyton in LC2 did not remain at the water surface after Day 1. The specific cause of this is not clear. We present the results below comparing the two pools but are not able to provide definitive conclusions on this aspect of the experiment. The present experiment was performed during November 2010, at which time the water depth in the immediate vicinity of the site and the average depth in the limnocorrals was 60 cm. Closer to the center of the slough, approximately 200 m from the limnocorrals, the water depth was on average 37.0 cm, standard deviation 8.9 cm over an area of 200 m^2. Thus, if the gas transfer velocity had been measured farther from the sawgrass, we would expect the change in gas concentration in the water with time to be greater if the value of k_{600} were the same as what was measured in this study.

3.2.2 Environmental parameters

It has been established that in a wetland environment such as the Everglades, the gas transfer velocity is primarily a function of wind speed (e.g. Cole and Caraco, 1998) and rain rate (e.g. Ho *et al.*, 1997). However, as there was no rainfall at the study site over the course of the experiment (6 - 9 November 2010), it was not necessary to measure this parameter.

In order to gain a basic understanding of the wind speed profile over water near a region of densely-growing sawgrass, two sonic anemometers (Gill Windmaster Pro) were mounted on the tripod at the study site. Anemometer #1 (A1) was situated 85 cm above the mean water line, below the average sawgrass height; anemometer #2 (A2) was located above the mean sawgrass height, at 3.0 m above the mean water line. A datalogger (Campbell Scientific CR-1000) was installed on the platform; A1 communicated via serial protocol with the datalogger, whereas A2 produced an analogue signal. Instantaneous wind speeds were logged, making it necessary to log data at a relatively high frequency (0.1 - 0.017 Hz) and average the resulting data over 15-minute intervals. Data from A1 were logged throughout the experimental period; however, data from A2 were logged only for three hours. A faulty electrical connection caused no further data to be recorded from A2. Therefore, we do not present results from A2 below but refer rather to 10-m wind speed measurements made at a nearby meteorological station (station S331W located 29 km from the study site, http://www.sfwmd.gov); this station was used for the same purpose by Hagerthey *et al.* (2010).

To determine the effect of the sawgrass on the wind speed profile, it was initially assumed that the sawgrass would have no effect, so the wind profile would be logarithmic with height. To extrapolate the 85-cm wind speeds to a reference height of 10 m while accounting for stability affects, it was necessary to monitor the air temperature, relative humidity, and water temperature, and to parameterize the drag coefficient as a function of wind speed. The former two parameters were measured by a Relative Humidity and Temperature probe (Vaisala HMP 50), which communicated with the datalogger. Water temperature was measured once per hour

during gas exchange experiments using an isoamyl benzoate thermometer with a precision of 1.0^o C. Temperatures were linearly interpolated over the course of each day to match the frequency of measurements logged by the CR-1000.

Wind speeds were extrapolated to a height of 10 m using the COARE algorithm, which includes a parameterization for the drag coefficient (Fairall *et al.*, 2003). Air pressure was assumed to be equal to that at a nearby USGS station, located at 26.612^o N, 80.033^o W. The downward shortwave and longwave radiation and planetary boundary height were taken to be constant (150 W m^{-2}, 370 W m^{-2}, and 600 m, respectively). The COARE model was not sensitive to these values and output the same extrapolated wind speeds when these values were within the given values $\pm$ 50%.

3.2.3 Gas tracer experiments

At the beginning of the experiment (Day 0), approximately 12 pmol of sulfur hexafluoride (SF_6), a biologically and chemically inert gas, were injected into each of the limnocorrals and gently mixed to ensure a constant concentration throughout each. Throughout Days 1 - 4, water in each limnocorral was sampled every hour for 5.5 - 7 hours using glass syringes. Syringes were kept under water in a cooler until transported to the laboratory for analysis that evening. On each day, sampling was done in triplicate in each corral, and the three samples were taken from at least two different locations to check that gas concentrations remained well-mixed. Each sample contained 30 mL water. Care was taken to ensure that no bubbles were present in the syringes by submerging each syringe completely when sampling.

The principle and mathematical derivation of the deliberate tracer gas evasion technique are described in Chapter 2 above and by Wanninkhof *et al.* (1987). The normalized gas transfer velocity is determined from the following equation, derived from Equations 2.2.8 and 2.2.9:

$$k_{600} = -h\frac{\Delta \ln\left([\mathrm{SF_{6,water}} - \alpha[\mathrm{SF_{6,air}})\right]}{\Delta t}\left(\frac{600}{\mathrm{Sc_{SF_6}}}\right)^{-n} \tag{3.2.1}$$

Here we take $n = \frac{2}{3}$ according to the smooth wall model of gas exchange. It has empirically been found that this is accurate for gas exchange at a smooth interface

free of waves, which was the case in this experiment (Deacon, 1977; Jähne *et al.*, 1984).

3.3 Results

3.3.1 Atmospheric stability

The stability of the boundary layer depends on the air temperature and relative humidity, as well as the underlying water temperature. Using the COARE algorithm and specifically the stability parameter ζ, we determined that atmospheric conditions were unstable during Day 1, but were stable during experiments on Days 2 - 4. In the case of each experiment, the relative humidity follows the inverse of the air temperature trend over the course of the day, as expected. These data suggest that there was relatively little evaporation from the pools compared to the total volume over these time scales, as relative humidity decreased as the temperature rose.

In each of the latter experiments, the water temperature was cooler than the air temperature, typically by 2 - 3^o C (see Figure 3.2). Experiments 2 & 3 ended approximately at the time of peak air temperature, evidenced by the decrease in slope; the air temperature and relative humidity data collection were terminated early due to loss of power at the site during experiment 4. It is possible that conditions were convectively unstable during the evenings, as the air cools more rapidly than the water, but no experiments were carried out during these times.

3.3.2 Wind speeds

Wind speeds over the duration of the experiment measured at 10 m above the water surface at a nearby meteorological station and at 85 cm at the study site are shown in Figure 3.3, averaged over 15 minute intervals. It is important to note that these experiments were conducted during a period of relatively high wind speeds for this region, ranging from 3.1 - 6.0 m s^{-1}. As expected, the 85-cm wind speeds are typically lower than the 10-m wind speed measurements. While it is likely that there is a small spatial gradient in the 10-m wind speed between the study site and the

station (a distance of 29 km), we assume for our purposes that the 10-m wind speed is the same at these two locations. This is the assumption that was made by Hagerthey *et al.* (2010) in predicting gas transfer velocities based on wind speed. Because of the nonlinear relationship between wind speed and gas transfer velocity, we account for the gas exchange enhancement due to wind speed variability by calculating the RMS wind speed for each experiment. This is mathematically equivalent to the approach of Wanninkhof *et al.* (2007), who assumed that the gas transfer velocity is proportional to u_{10}^2 and therefore used the second moment of the wind speed, M_2, to calculate the predicted gas transfer velocity: $k_{600} = aM_2$. The second moment, M_2, is defined as $M_2 = \sum(u_{10}^2)N^{-1}$, where N represents the number of points in the averaging interval. Thus, $M_2 = u_{\mathrm{rms}}^2$. We use u_{rms} rather than M_2 here because CC98 and W92 predict that the gas transfer velocity is proportional to the wind speed to a power close to but not equal to 2. This approach is used to compare these parameterizations to the data, as well as to construct the best-fit parameterization to these data below.

In examining the effect of the sawgrass on the wind speed profile, we compare a possible idealized wind speed profile based on experimental data from Raupach *et al.* (1996) above and in a vegetation canopy to the profile derived from the 85-cm wind speed measurement and the COARE algorithm (see Figure 3.4). While an average 10-m wind speed of 6.0 m s^{-1} was measured on Day 1, the 85-cm wind speed was 4.7 m s^{-1}, yielding a predicted 10-m wind speed of only 5.2 m s^{-1}. This difference is smaller than what might be expected from a measurement closer to the sawgrass or closer to the water surface. The discrepancy between the measured u_{10} and the value extrapolated from the 85-cm measurement is most likely due in part to a difference in the drag coefficient near the sawgrass but also to a change in the wind speed profile, as the presence of a vegetation canopy would most likely alter not only u_* and z_0 but also cause the logarithmic profile approximation to no longer hold. The comparison of these wind speeds and the friction velocity is discussed in more detail below. It is important to note that on the days of lowest wind speed, the extrapolated values of u_{10} are higher than, though still within one standard deviation of the measured 10-m wind speed. Physically, we expect the actual u_{10} to be higher than what would

be predicted by a logarithmic profile; possible causes of error in this comparison are discussed in the following section.

3.3.3 Gas transfer velocities

A summary of the gas transfer velocities and environmental parameters is presented in Table 3.1. While the averaged 10-m wind speeds ranged from 3.1 - 6.0 m s^{-1}, the measured gas transfer velocities varied from 0.8 - 2.0 cm h^{-1}. With the exception of the data from Day 1, the gas transfer velocity appears to scale with the 10-m wind speed to the power of 1.38. As discussed above, however, the conditions for experiment 1 were anomalous in multiple respects: the edge of the limnocorral was lowered after experiment 1 in order to less obstruct the wind profile, and the COARE stability parameter indicated unstable conditions during this period. Therefore, the gas transfer velocity data from this day has been excluded in further analysis below in comparing this experiment with the remaining three.

In these experiments, the errorbars, determined from the product of the water depth and the standard error in the slope of the logarithm of the change in SF_6 concentration over time, are significant (10 - 41%). Typically, the standard error is approximately 10 - 25% for gas transfer velocities in this range in laboratory experiments using the deliberate tracer injection method (e.g. Ho *et al.*, 2007; Harrison *et al.*, in prep, also see Chapter 2). The higher errorbars in this experiment may result from a lack of thorough mixing in each limnocorral, which is likely at such low gas transfer velocities but is accounted for by sampling at multiple locations in each limnocorral. Figure 3.5 depicts the eight gas transfer velocities measured in the two limnocorrals over the course of the four experiments, with the associated standard errors.

Gas exchange parameterization

Figure 3.6 shows the gas transfer velocities measured in this experiment plotted as a function of wind speed. It is evident that both CC98 and W92 predict significantly higher gas transfer velocities at corresponding wind speeds. At $u_{10} = 3.1$

m s^{-1}, CC98 over-predicts the gas transfer velocity by 320%, while W92 over-predicts the measured k_{600} by 240%; at high wind speeds measured in this study, the gas transfer velocity is over-estimated by 220% and 310% by CC98 and W92, respectively. Possible reasons for these over-predictions are discussed in more detail below. Plotted in Figure 3.6 as well (red line) is the best-fit power law function relating k_{600} to u_{10} for the data from the present study:

$$k_{600} = 0.176 \cdot u_{10}^{1.38} \tag{3.3.1}$$

This parameterization is not intended to substitute for CC98 or W92, as there are possible shortcomings in the experimental setup that this does not take into account; additionally, it is logical to use the friction velocity rather than the 10-m wind speed to parameterize k_{600}. Both of these points are discussed in more detail below.

3.3.4 Effects of periphyton on gas exchange

Water from the two limnocorrals was sampled concurrently to determine the effect of periphyton on the gas transfer velocities; these comparisons are shown in Figure 3.5. The corral free of periphyton is denoted as LC1, while LC2 contained a significant amount of organic matter. As discussed above, although the periphyton included floral species that initially floated at the water surface, they ceased to float after Day 1. In each experiment, the gas transfer velocity measured in LC1 exceeded that of LC2. However, because of the relatively low gas transfer velocities and relatively high errors involved in this measurement and calculation, k_{600} was not significantly higher in LC1 compared to LC2. The one exception to this was experiment 3, in which the standard error was low, allowing us to distinguish between gas transfer velocities in the two limnocorrals. On Day 3, k_{600} in LC1 was measured to be 1.45 $\pm$ 0.15 cm h^{-1}, and k_{600} in LC2 was 1.03 $\pm$ 0.24 cm h^{-1}.

Because the periphyton ceased to float at the water surface in LC2 after Day 1, it is impossible to attribute the measured differences in gas transfer velocity to the physical obstruction of macrophytes floating at the surface. The limnocorrals were adjacent to each other, making it unlikely that the platform would have shielded one limnocorral from the wind more so than the other, so it is also unlikely that

this would explain the difference in gas transfer velocities. While it is probable that the water in both limnocorrals contained surfactants due to the fact that this is a highly eutrophic region of the Everglades, it is possible that the periphyton in LC2 continued to produce compounds that increased the surface film concentration over the course of the experiments, thus reducing the gas exchange somewhat in LC2, in comparison to LC1, where the surfactant concentration may have remained constant. No measurements of surfactant concentration were made in either corral during these experiments, so we are not able to definitively conclude the cause of this trend in the data. We therefore present no further analysis of these data and use only gas transfer velocities from LC1 in further analysis and discussion.

3.4 Discussion

3.4.1 Sawgrass and wind speed profile

While many studies to date have investigated flow patterns inside vegetation canopies (see, for example, Finnigan, 2000, and references therein), the wind profile within a few meters horizontally of the canopy is likely to be somewhat more complicated, due to the turbulent wake generated by wind passing over the sawgrass. For simplicity, we allow our null hypothesis to be that the effect of the sawgrass on both the wind profile and drag coefficient is negligible at the location of the anemometer, approximately 2 m from the sawgrass edge. Following this assumption, we apply the COARE algorithm to extrapolate from the 85-cm measurement of wind speed to the 10-m wind speed expected based on a logarithmic profile and parameterizing the drag coefficient as a function of wind speed. Except on Days 3 and 4, when the wind speed was relatively low ($u_{10} = 3.1 - 4.6$ m s^{-1}), the measured 10-m wind speed was greater than the extrapolated 10-m wind speed. On each day, however, if the standard deviation in the wind speeds is taken into account, the difference between the extrapolated and measured u_{10} values is not statistically significant. This is most likely due to the fact that these calculations are based on instantaneous measurements, and the wind speed varied during each experiment. Additionally, the wind

speed profile at a given instant will not be exactly logarithmic; this is simply a statistical approximation, which may account for a significant portion of the error in this wind speed comparison. It is important to determine u_{10} accurately, however, as this has implications for the predicted gas transfer velocities, due to the fact that k_{600} is typically parameterized in terms of u_{10}; this is discussed in more detail below.

The most important difference in the profiles shown in Figure 3.4 relating to gas exchange is the difference in the friction velocities in the two profiles. The friction velocity, u_*, is defined in terms of the shear stress at the surface, τ, and the density of air, ρ_a: $u_* = \sqrt{\tau/\rho_a}$. If a logarithmic wind speed profile is assumed, the surface stress and, hence, friction velocity would be estimated to be much greater than in the case of the idealized wind speed profile shown here. It is the shear stress at the surface, not the wind at 10 m above the water surface, that governs air-water gas exchange. Over the open ocean, it is typically assumed that the drag coefficient can be parameterized as a function of u_{10}, and, as $u_* = u_{10}\sqrt{\mathrm{C_D}}$, the friction velocity can therefore be estimated directly from u_{10}. However, we have demonstrated here that common parameterizations for the drag coefficient do not hold in an environment with vegetation obstructing the wind near the water surface.

As evidenced by the discrepancy in the extrapolated and measured values of u_{10}, it is clear that the wind stress at the water surface may not be easily correlated with the 10-m wind speed in this type of wetland environment. It therefore would be logical to follow Jähne *et al.* (1979) and to parameterize the gas transfer velocity in terms of the friction velocity rather than u_{10}. As we have measured wind speeds only at one height above the water surface in the present experiment, it is impossible to provide a more detailed functional analysis of the actual wind speed profile below the sawgrass height; we therefore cannot determine the surface stress or the friction velocity in this case. Future experiments should monitor the wind speeds at several heights above the water surface and below the height of the vegetation to gain a better understanding of this profile. Additionally, it would be instructive to collect profiles at several locations at different horizontal distances from the edge of the sawgrass. In the middle of a slough, for example, it is possible that a logarithmic wind profile

approximation would hold, if the slough is sufficiently large. Close to the sawgrass, our data indicate that, as expected, this approximation may no longer hold.

3.4.2 Gas transfer velocity parameterization

The data shown in Figure 3.6 depict gas transfer velocities measured in LC1. The parameterizations plotted on the same axes represent best fit curves suggested by Cole and Caraco (1998) and Wanninkhof (1992), and are both based on previous field measurements of k_{600} in lakes, estuaries, or other freshwater environments. It is clear in this experiment, however, that both CC98 and W92 over-predict the gas transfer velocity based on the wind speeds as inferred in this study. As these data were collected during a high wind period in the Everglades and typical wind speeds are lower than the results presented here, it appears that W92 may be more appropriate to use at this site during periods when fluxes due to thermal convection are negligible, as the error is smaller at lower wind speeds. Because no experiments were conducted during periods of high buoyancy flux, we cannot draw a conclusion regarding the gas transfer velocity during such periods. The functionality of the parameterization for the data presented here has been chosen to match that of W92, which neglects the effect of buoyancy fluxes at low wind speeds. This may or may not be accurate, but further study is required at this site at low wind speeds to determine this.

With reference to the study conducted by Hagerthey *et al.* (2010), our results show that assuming the relationship for the gas transfer velocity proposed by Cole and Caraco (1998) could have significant implications for the calculated metabolic rates. For example, if wind speeds average 3 m s^{-1}, CC98 over-predicts the gas transfer velocity by 330%, based on the trend inferred from the results in this study. This could cause an over-prediction of the rates of gross and net primary production (GPP and NPP, respectively) on the order of 80 mmol O_2 m^{-2} d^{-1}, corresponding to 17% and 35% of the GPP and NPP predicted by the gas transfer velocities found in this study. This calculation is based on the assumption that the O_2 concentration, O_2 saturation, change in O_2 concentration in the water with time, and rate of respiration

were 4 g L^{-1}, 50%, 255 mmol O_2 m^{-2} d^{-1}, and 250 mmol O_2 m^{-2} d^{-1}, respectively. This assumption is representative of the data in the study.

A few notes should be made about the gas transfer velocity measurements made here. First and most important, because the wind speed profile is probably not logarithmic, the wind speed measured at 10 m above the water surface does not correlate clearly with a given friction velocity. Indeed, at different distances from the sawgrass, it is likely that the friction velocity may differ even if the value of u_{10} is constant, due to variations in the wind profile, discussed above. Furthermore, if the wind speed is measured at a height other than 10 m, unless the wind profile is well-characterized by several wind speed measurements above the sawgrass height, it is not possible to accurately extrapolate the measurement to determine the appropriate u_{10}. It is of note, however, that due to a high buoyancy flux dependence (predicted gas transfer velocity in the absence of wind), CC98 over-predicts the gas transfer velocity regardless of the wind speed. It appears that instead of using u_{10} to predict the gas transfer velocities, parameterizations should be recast in terms of the friction velocity, and u_* should be measured in order to describe the gas transfer velocity more accurately.

Second, our air and water temperature and relative humidity data indicate that the atmospheric conditions were stable during experiments on Days 2 - 4. This would explain the apparently low influence of the aforementioned buoyancy flux due to thermal convection and hence lower than predicted gas transfer velocities, though it is also possible that the effect of the buoyancy flux would not be measurable at these wind speeds. If it is assumed that buoyancy fluxes do not play a role in the gas transfer velocity and the y-intercept of CC98 is neglected, the resulting parameterization over-predicts the measured gas transfer velocities by 390 - 990% along the wind speed domain here. It would be useful to conduct experiments during convectively unstable conditions as well to compare the gas transfer velocity results during periods of similar wind speeds and determine the relative contributions of the wind and buoyancy fluxes to gas exchange enhancement.

Third, as mentioned above, it was evident that the edges of the limnocorrals were obstructing the wind profile near the water surface during the experiment on

Day 1, and they were subsequently deflated somewhat. It is possible, however, that the edges continued to disrupt the wind speed profile near the surface, lowering the surface turbulence and hence the gas transfer velocity in the limnocorrals. As the edge of the limnocorral acts as a barrier between the water outside and the inside the corral, it is a necessity; however, it would be instructive to decrease the extent of the barrier in increments to determine the gas transfer velocity in the limiting case in which there is no barrier.

Fourth, it is of note that the results from this study represent gas transfer velocities measured in close proximity to the sawgrass surrounding the slough. Based on the typical size of a non-deteriorated slough in the ridge and slough landscape of approximately 650 m North to South and 250 m East to West (Wu *et al.*, 2006), only 1% of the water surface is within 2 m of the surrounding sawgrass. It is possible that these data are strictly representative of only a small area, as near-surface wind speeds may be higher at the center of the slough, causing greater enhancement of turbulence and gas exchange. Therefore, averaging the gas transfer velocity over the entire volume of the slough may cause the estimated gas flux to increase.

A final proposed explanation for the over-prediction of the gas transfer velocity by the two parameterizations shown here is the influence of surfactants in reducing surface turbulence and hence gas exchange. We did not quantify surfactant concentration in this experiment, though it is likely that surface films were present due to the high biomass in the water, and surface films are known to reduce the gas transfer velocity. Further experiments in different regions of the Everglades (i.e. eutrophic and oligotrophic) should measure the surface tension as it is likely that the dependence of the gas transfer velocity on wind speed differs, perhaps significantly (Frew *et al.*, 1990), between these types of environments.

3.5 Summary and Conclusions

In this study, we found that 10-m wind speeds between 3.1 and 5.8 m s^{-1} enhance the gas transfer velocity in a slough region of the Everglades near sawgrass to approximately 0.8 - 2.0 cm h^{-1}. This range of values of k_{600} in this wind speed

domain is significantly lower than what would be predicted by common gas transfer velocity parameterizations, including CC98 and W92.

The fact that CC98 and W92 both over-predict the measured gas transfer velocities in this environment may be due in part to the dense sawgrass in the vicinity of the experimental setup, which may act to shield the surface water from the wind stress by reducing the friction velocity at the air-water interface. The value of u_* has not been determined in these experiments due to lack of sufficient data and a full wind speed profile below the sawgrass height; however, the friction velocity has been used to parameterize the gas transfer velocity in other studies, and it may hold the most promise for this type of setting where vegetation obstructs the wind profile.

Taking into consideration possible shortcomings in the experimental setup, it is possible that surfactants play a role in depressing the gas transfer velocity, possibly significantly, in this eutrophic area in the Everglades, which is located in a degraded ridge and slough region where periphyton is present in abundance. As direct measurements of surfactant concentration were not conducted in this experiment, it is not possible to ascertain this at this time, though this would explain the over-prediction of the gas transfer velocities at the measured wind speeds by CC98 and W92. Future studies should quantify the concentration of surfactants, as it appears that this may have significant implications for studies parameterizing gas exchange in the Everglades.

Figure 3.1: Platform, one limnocorral, and tripod with anemometers (85 cm and 3.0 m above water level) used in present experiment

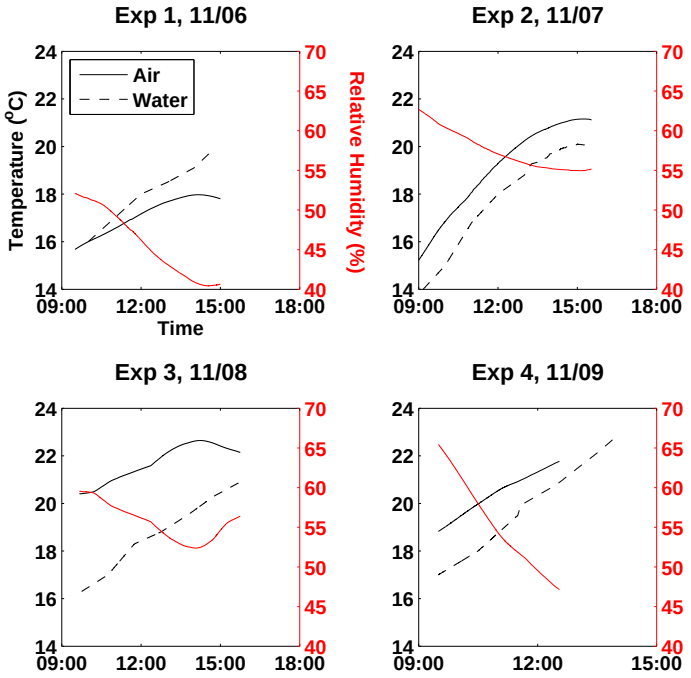

Figure 3.2: Air and water temperature and relative humidity over the course of the experiment

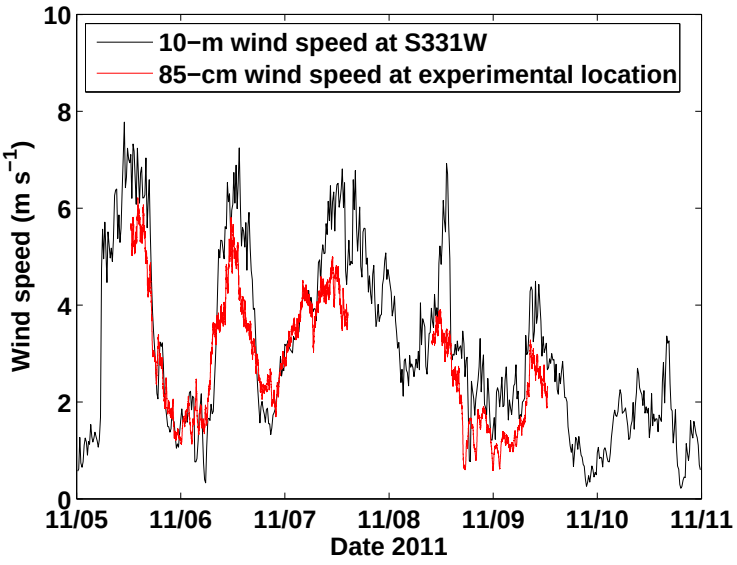

Figure 3.3: Wind speeds measured at a nearby meteorological station (S331W) at 10 m and at the study site at 85 cm above the water surface

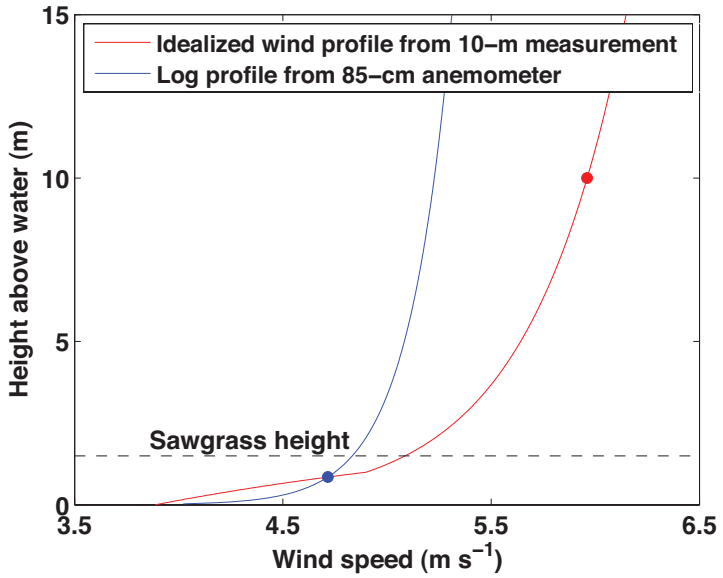

Figure 3.4: An idealized wind speed profile near the sawgrass based on the true 10-m wind speed during Day 1 compared to the extrapolated wind speed profile based on the 85-cm wind speed and the COARE algorithm; highlight points show measured wind speeds

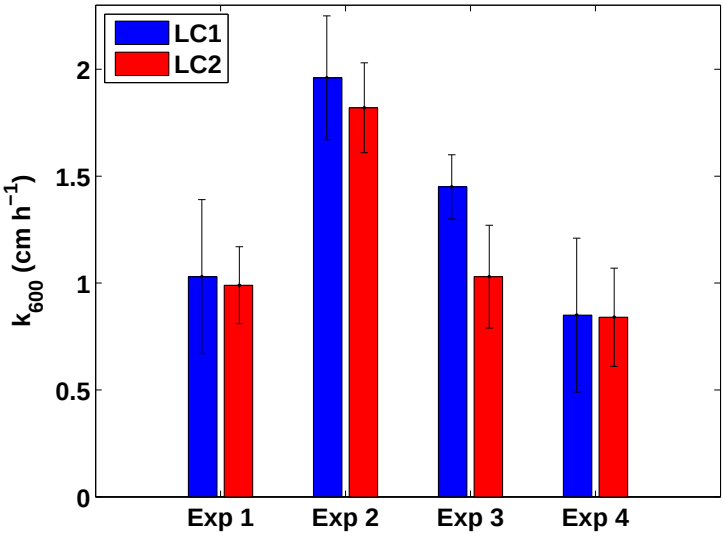

Figure 3.5: Gas transfer velocities measured in limnocorrals 1 and 2 over the four days of the experiment. Error bars show standard error for each calculated value

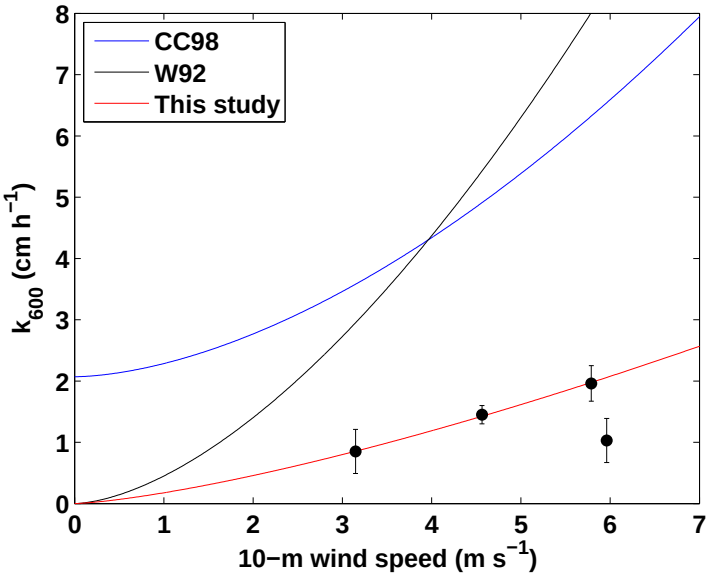

Figure 3.6: Gas transfer velocity plotted against 10-m wind speed, measured at station S331W. Common parameterizations are shown predicting gas transfer velocity from the 10-m wind speed, including a best-fit parameterization for the present data (red line)

Exp	Date 2010	Duration (h)	Temperature (air) (^{o} C)	Temperature (water) (^{o} C)	Relative humidity (%)
1	06 Nov	5.5	17.1	18.0	45.7
2	07 Nov	7	18.5	17.1	58.2
3	08 Nov	6.5	21.7	18.8	55.6
4	09 Nov	6.5	20.1	18.7	57.3

Exp	10-m wind speed (m s^{-1})	Extrapolated u_{10} (m s^{-1})	k_{600} (cm h^{-1})	
			LC1	LC2
1	6.0 ± 0.6	5.2 ± 1.8	1.03 ± 0.36	0.99 ± 0.18
2	5.8 ± 0.7	5.6 ± 1.5	1.96 ± 0.29	1.82 ± 0.21
3	4.6 ± 1.2	4.8 ± 1.6	1.45 ± 0.15	1.03 ± 0.24
4	3.1 ± 0.6	3.7 ± 1.0	0.85 ± 0.36	0.84 ± 0.23

Table 3.1: Atmospheric parameters (averaged) and gas transfer velocities measured throughout experiment; 10-m wind speed was measured at station S331W and the extrapolated u_{10} is derived from the 85-cm wind speed measurements and the COARE algorithm

Bibliography

Anis, A., and J. N. Moum, 1995: Surface wave-turbulence interactions: Scaling ϵ(z) near the sea surface. *J. Phys. Oceanogr.*, **25**, 2025 – 2045.

Asher, W. E., and P. J. Farley, 1995: Phase-Doppler anemometer measurement of bubble concentrations in laboratory-simulated breaking waves. *J. Geophys. Res.*, **100**, C4, 7045 – 7056.

Asher, W. E., L. M. Karle, and B. J. Higgins, 1997: On the differences between bubble-mediated air-water transfer in freshwater and seawater. *J. Mar. Res.*, **55**, 813 – 845.

Asher, W. E., L. M. Karle, B. J. Higgins, P. J. Farley, E. C. Monahan, and I. S. Leifer, 1996: The influence of bubble plumes on air-seawater gas transfer velocities. *J. Geophys. Res.*, **101**, C5, 12,027 – 12,041.

Asher, W. E., and J. F. Pankow, 1986: The interaction of mechanically generated turbulence and interfacial films with a liquid phase controlled gas/liquid transport process. *Tellus*, **38B**, 305 – 318.

Banks, R. B., G. B. Wickramanayake, and B. N. Lohani, 1984: Effect of rain on surface reaeration. *J. Environ. Eng.*, **110**, 1 – 14.

Bates, T. S., K. C. Kelly, and J. E. Johnson, 1993: Concentrations and fluxes of dissolved biogenic gases (DMS, CH_4, CO, CO_2) in the Equatorial Pacific during the SAGA 3 experiment. *J. Geophys. Res.*, **98**, D9, 16,969 – 16,977.

Bliven, L. F., N. E. Huang, and S. R. Long, 1984: A laboratory study of the velocity field below surface gravity waves. *Gas Transfer at Water Surfaces*, W. Brutsaert and G. H. Jirka, eds., D. Reidel Publishing Company, Hingham, MA, 181 – 190.

Bock, E. J., T. Hara, N. M. Frew, and W. R. McGillis, 1999: Relationship between air-sea gas transfer and short wind waves. *J. Geophys. Res.*, **104**, C11, 25,821 – 25,831.

Bopp, R. F., 1983: Revised parameters for modeling the transport of PCB components across an air water interface. *J. Geophys. Res.*, **88**, C4, 2521 – 2529.

Borges, A. V., and R. Wanninkhof, 2007: 37th International Liège Colloquium on Ocean Dynamics, Liège, Belgium, May 2 – 6, 2005, 5th International Symposium on Gas Transfer At Water Surfaces. *J. Mar. Syst.*, **66**, 1 – 3.

Broecker, H.-C., J. Peterman, and W. Siems, 1978: The influence of wind on CO_2-exchange in a wind-wave tunnel, including the effects of monolayers. *J. Mar. Res.*, **36**, 595 – 610.

Broecker, W. S., and T.-H. Peng, 1971: The vertical distribution of radon in the BOMEX area. *Earth Planet. Sci. Lett.*, **11**, 99 – 108.

Broecker, W. S., T.-H. Peng, G. Ostlund, and M. Stuiver, 1985: The distribution of bomb radiocarbon in the ocean. *J. Geophys. Res.*, **90**, C4, 6953 – 6970.

Brumley, B. H., and G. H. Jirka, 1988: Air water transfer of slightly soluble gases: Turbulence, interfacial processes and conceptual models. *PhysicoChemical Hydrodynamics*, **10**, 295 – 319.

Businger, J. A., J. C. Wungaard, Y. Izumi, and E. F. Bradley, 1971: Flux-profile relationships in the atmospheric surface layer. *J. Atmos. Sci.*, **28**, 181 – 189.

Caffrey, J. M., 2004: Factors controlling net ecosystem metabolism in U. S. estuaries. *Estuaries*, **27**, 90 – 101.

Cember, R., 1989: Bomb radiocarbon in the Red Sea: A medium-scale gas exchange experiment. *J. Geophys. Res.*, **94**, C2, 2111 – 2123.

Clark, J. F., P. Schlosser, R. Wanninkhof, H. J. Simpson, W. S. F. Schuster, and D. T. Ho, 1995: Gas transfer velocities for SF_6 and ^3He in a small pond at low wind speeds. *Geophys. Res. Lett.*, **22**, 93 – 96.

Cole, J. J., and N. F. Caraco, 1998: Atmospheric exchange of carbon dioxide in a low-wind oligotrophic lake measured by the addition of SF_6. *Limnol. Oceanogr.*, **43**, 647 – 656.

Cole, J. J., Y. T. Prairie, N. F. Caraco, W. H. McDowell, L. J. Tranvik, R. G. Striegl, C. M. Duarte, P. Kortelainen, J. A. Downing, J. J. Middelburg, and J. Melack, 2007: Plumbing the global carbon cycle: Integrating inland waters into the terrestrial carbon budget. *Estuaries*, **10**, 171 – 184, doi:10.1007/s10021-006-9013-8.

Csanady, G. T., 1990: The role of breaking wavelets in air-sea gas transfer. *J. Geophys. Res.*, **95**, C1, 749 – 759.

Danckwerts, P. V., 1970: *Gas-Liquid Reactions*. McGraw-Hill Book Company, San Francisco, CA.

Deacon, E. L., 1977: Gas transfer to and across an air-water interface. *Tellus*, **29**, 363 – 374.

Dillon, T. M., J. G. Richman, C. G. Hansen, and M. D. Pearson, 1981: Near surface turbulence measurements in a lake. *Nature*, **290**, 390 – 392.

Fairall, C. W., E. F. Bradley, J. E. Hare, A. A. Grachev, and J. B. Edson, 2003: Bulk parameterization of air-sea fluxes: Updates and verification for the COARE algorithm. *J. Climate*, **16**, 571 – 591.

Fairall, C. W., A. B. White, J. B. Edson, and J. E. Hare, 1997: Integrated shipboard measurements of the marine boundary layer. *J. Atmos. Oceanic Tech.*, **14**, 338 – 359.

Farmer, D. M., C. L. McNeil, and B. D. Johnson, 1993: Evidence for the importance of bubbles in increasing air-sea gas flux. *Nature*, **361**, 620 – 623.

Finnigan, J., 2000: Turbulence in plant canopies. *Annu. Rev. Fluid Mech.*, **32**, 519 – 571.

Forster, P., V. Ramaswamy, P. Artaxo, T. Berntsen, R. Betts, D. W. Fahey, J. Haywood, J. Lean, D. C. Lowe, G. Myhre, J. Nganga, R. Prinn, G. Raga, M. Schulz, and R. Van Dorland, 2007: Changes in Atmospheric Constituents and in Radiative Forcing. *Climate Change 2007: The Physical Science Basis*, S. Solomon, D. Qin, D. M. Manning, Z. Chen, M. Marquis, K. B. Averyt, M. Tignor, and H. L. Miller, eds., Cambridge University Press, New York, NY.

Frew, N. M., E. J. Bock, U. Schimpf, T. Hara, H. Haußecker, J. B. Edson, W. R. McGillis, R. K. Nelson, S. P. McKenna, B. M. Uz, and B. Jähne, 2004: Air-sea gas transfer: Its dependence on wind stress, small-scale roughness, and surface films. *J. Geophys. Res.*, **109**, C08S17, doi:10.1029/2003JC002131.

Frew, N. M., J. C. Goldman, M. R. Dennett, and A. S. Johnson, 1990: Impact of phytoplankton-generated surfactants on air-sea gas exchange. *J. Geophys. Res.*, **95**, C3, 3337 – 3352.

Green, T., and D. F. Houk, 1979: The mixing of rain with near-surface water. *J. Fluid Mech.*, **90**, 569 – 588.

Gunn, R., and G. Kinzer, 1949: The terminal velocity of fall for water droplets in stagnant air. *J. Meteor.*, **6**, 243 – 248.

Hagerthey, S. E., J. J. Cole, and D. Kilbanea, 2010: Aquatic metabolism in the Everglades: Dominance of water column heterotrophy. *Limnol. Oceanogr.*, **55**, 653 – 666.

Harrison, E. L., F. Veron, D. T. Ho, M. C. Reid, S. S. Eggleston, P. Orton, and W. R. McGillis: Nonlinear interaction between rain and wind induced air-water gas exchange, *J. Geophys. Res.*, in prep.

Higbie, R., 1935: The rate of absorption of a pure gas into a still liquid during short periods of exposure. *Trans. Am. Inst. Chem. Engrs.*, **35**, 360 – 365.

Ho, D. T., W. E. Asher, L. F. Bliven, P. Schlosser, and E. L. Gordan, 2000: On mechanisms of rain-induced air-water gas exchange. *J. Geophys. Res.*, **105**, C10, 24,045 – 24,057.

Ho, D. T., L. F. Bliven, R. Wanninkhof, and P. Schlosser, 1997: The effect of rain on air-water gas exchange. *Tellus*, **49**, 149 – 158.

Ho, D. T., C. S. Law, M. J. Smith, P. Schlosser, M. Harvey, and P. Hill, 2006: Measurements of air-sea gas exchange at high wind speeds in the Southern Ocean: Implications for global parameterizations. *Geophys. Res. Lett.*, **33**, L16611, doi:10.1029/2006GL026817.

Ho, D. T., P. Schlosser, and P. M. Orton, 2011a: On factors controlling air-water gas exchange in a large tidal river. *Estuaries and Coasts*, 1 – 14, doi:10.1007/s12237-011-9396-4.

Ho, D. T., F. Veron, E. Harrison, L. F. Bliven, N. Scott, and W. R. McGillis, 2007: The combined effect of rain and wind on air-water gas exchange: A feasibility study. *Journal of Marine Systems*, **66**, 150 – 160.

Ho, D. T., R. Wanninkhof, P. Schlosser, D. S. Ullman, D. Hebert, and K. F. Sullivan, 2011b: Towards a universal relationship between wind speed and gas exchange: Gas transfer velocities measured with $^3He/SF_6$ during the Southern Ocean Gas Exchange Experiment. *J. Geophys. Res.*, **116**, C00F04, doi:10.1029/2010JC006854.

Ho, D. T., C. J. Zappa, W. R. McGillis, L. F. Bliven, B. Ward, J. W. H. Dacey, P. Schlosser, and M. B. Hendricks, 2004: Influence of rain on air-sea gas exchange: Lessons from a model ocean. *J. Geophys. Res.*, **109**, C08S18, doi::10.1029/2003JC001806.

Jähne, B., W. Huber, A. Dutzi, T. Wais, and J. Ilmberger, 1984: Wind wave-tunnel experiment on the Schmidt number - and wave field dependence of air/water gas exchange. *Gas Transfer at Water Surfaces*, W. Brutsaert and G. H. Jirka, eds., D. Reidel Publishing Company, Hingham, MA, 303 – 309.

Jähne, B., P. Libner, R. Fischer, T. Billen, and E. J. Plate, 1989: Investigating the transfer processes across the free aqueous viscous boundary layer by the controlled flux method. *Tellus*, **41B**, 177 – 195.

Jähne, B., K. O. Münnich, and O. Siegenthaler, 1979: Measurements of gas exchange and momentum transfer in a circular wind-water tunnel. *Tellus*, **31**, 321 – 329.

Jähne, B., T. Wais, L. Memery, G. Caulliez, L. Merlivat, K. O. Münnich, and M. Coantic, 1985: He and Rn gas exchange experiments in the large wind-wave facility of IMST. *J. Geophys. Res.*, **90**, C6, 11,989 – 11,997.

Jones, E. P., and S. D. Smith, 1977: A first measurement of sea-air CO_2 flux by eddy correlation. *J. Geophys. Res.*, **82**, 5990 – 5992.

Kitaigorodskii, S. A., and M. A. Donelan, 1984: Wind-wave effects on gas transfer. *Gas Transfer at Water Surfaces*, W. Brutsaert and G. H. Jirka, eds., D. Reidel Publishing Company, Hingham, MA, 147 – 170.

Komori, S., N. Takagaki, R. Saiki, N. Suzuki, and K. Tanno, 2007: The Effect of raindrops on interfacial turbulence and air-water gas transfer. *Transport at the Air-Sea Interface*, C. S. Garbe, R. A. Handler, and B. Jähne, eds., Springer Berlin Heidelberg, 169 – 179.

Ledwell, J. J., 1984: The Variation of the Gas Transfer Velocity with Molecular Diffusivity. *Gas Transfer at Water Surfaces*, W. Brutsaert and G. H. Jirka, eds., D. Reidel Publishing Company, Hingham, MA, 293 – 302.

Lindberg, S. E., and H. Zhang, 2000: Air/water exchange of mercury in the Everglades II: measuring and modeling evasion of mercury from surface waters in the Everglades Nutrient Removal Project. *Sci. Total Environ.*, **259**, 135 – 143.

Liss, P. S., 1983: Gas transfer: Experiments and geochemical implications. *Air-Sea Exchange of Gases and Particles*, P. S. Liss and W. G. N. Slinn, eds., Reidel Publishing Company, Boston, MA, 241 – 298.

Liss, P. S., and L. Merlivat, 1986: Air-sea gas exchange rates: Introduction and synthesis. *The Role of Air-Sea Gas Exchange in Geochemical Cycling*, P. Buat-Ménard, ed., Reidel Publishing Company, Boston, MA, 113 – 129.

Livingstone, D. M., and D. M. Imboden, 1993: The non-linear influence of wind-speed variability on gas transfer in lakes. *Tellus*, **45B**, 275 – 295.

MacIntyre, S., R. Wanninkhof, and J. P. Chanton, 1995: Trace gas exchange across the air-water interface in freshwaters and coastal marine environments. *Biogenic trace gases: Measuring emissions from soil and water*, P. A. Matson and R. C. Harriss, eds., Blackwell, Cambridge, MA, 52 – 97.

Marshall, J. S., and W. M. Palmer, 1948: The distribution of raindrops with size. *J. Meteor.*, **5**, 165 – 166.

McConnell, L. L., W. E. Cothem, and T. F. Bidleman, 1993: Gas exchange of hexachlorocyclohexane in the Great Lakes. *Environ. Sci. Technol.*, **27**, 1304 – 1311.

McGillis, W. R., J. B. Edson, J. D. Ware, J. W. H. Dacey, J. E. Hare, C. W. Fairall, and R. Wanninkhof, 2001: Carbon dioxide flux techniques performed during GasEx-98. *Mar. Chem.*, **75**, 267 – 280.

Medwin, H., A. Kurgan, and J. A. Nystuen, 1990: Impact and bubble sound from raindrops at normal and oblique incidence. *Geophys. Res. Lett.*, **37**, L24604, doi:10.1029/2010GL044164.

Merlivat, L., and L. Memery, 1983: Gas exchange across an air-water interface: Experimental results and modeling of bubble contribution to transfer. *J. Geophys. Res.*, **88**, C1, 707 – 724.

Monin, A. S., and A. M. Obukhov, 1954: Dimensionless characteristics of turbulence in the surface layer. *Akad. Nauk SSSR, Geofiz. Inst., Tr.*, **24**, 163 – 187.

Naegler, T., P. Ciais, K. Rodgers, and I. Levin, 2006: Excess radiocarbon constraints on air-sea gas exchange and the uptake of CO_2 by the oceans. *Geophys. Res. Lett.*, **33**, L11802, doi:10.1029/2005GL025408.

Nightingale, P. D., G. Malin, C. S. Law, A. J. Watson, P. S. Liss, M. I. Liddicoat, J. Boutin, and R. C. Upstill-Goddard, 2000: In situ evaluation of air-sea gas exchange parameterizations using novel conservative and biological tracers. *Global Biogeochem. Cycles*, **14**, 373 – 387.

Ocampo-Torres, F. J., and M. A. Donelan, 1994: Laboratory measurements of mass transfer of carbon dioxide and water vapour for smooth and rough flow conditions. *Tellus*, **46B**, 16 – 32.

— 1995: On the influence of fetch and wave field on the co_2 transfer process: Laboratory measurements. *Air-Water Gas Transfer*, B. Jähne and E. C. Monahan, eds., Aeon Verlag, Heidelberg, 543 – 552.

Odum, H. T., 1956: Primary production in flowing waters. *Limnol. Oceanogr.*, **1**, 102 – 117.

Panofsky, H. A., and J. A. Dutton, 1984: *Atmospheric Turbulence*. Wiley-Interscience, Hoboken, NJ.

Pierrot, D., C. Neill, K. Sullivan, R. Castle, R. Wanninkhof, H. Lüger, T. Johannessen, A. Olsen, R. A. Feeley, and C. E. Cosca, 2009: Recommendations for autonomous underway pCO_2 measuring systems and data-reduction routines. *Deep-Sea Res. II*, **56**, 512 – 522.

Poon, Y.-K., S. Tang, and J. Wu, 1992: Interactions between rain and wind waves. *J. Phys. Oceanogr.*, **22**, 976 – 987.

Rathbun, R. E., 1979: *Estimating the gas and dye quantities for modified tracer technique measurements of stream reaeration coefficients*. U. S. Geological Survey Water-Resources Investigations, Reston, VA, 42 pp.

Raupach, M. R., J. J. Finnigan, and Y. Brunet, 1996: Coherent eddies and turbulence in vegetation canopies: the mixing layer analogy. *Bound.-Lay. Meteorol.*, **78**, 351 – 382.

Raymond, P. A., and J. J. Cole, 2001: Gas exchange in rivers and estuaries: Choosing a gas transfer velocity. *Estuaries*, **24**, 312 – 317.

Saylor, J. R., and R. A. Handler, 1999: Capillary wave gas exchange in the presence of surfactants. *Exp. Fluids*, **27**, 332 – 338.

Science Coordination Team, 2003: The role of flow in the Everglades ridge and slough landscape. *South Florida Ecosystem Restoration Working Group*, online at http://www.sfrestore.org/sct/docs/. Accessed July 2009.

Soloviev, A. V., and P. Schlüssel, 1994: Parameterization of the cool skin of the ocean and of the air-ocean gas transfer on the basis of modeling surface renewal. *Am. Met. Soc.*, **24**, 1339 – 1346.

Soloviev, A. V., N. V. Vershinsky, and V. A. Bezverchnii, 1988: Small scale turbulence measurements in the thin surface layer of the ocean. *Deep-Sea Res.*, **35**, 1859 – 1874.

Sweeney, C., E. Gloor, A. R. Jacobson, R. M. Key, G. McKinley, J. L. Sarmiento, and R. Wanninkhof, 2007: Constraining global air-sea exchange for CO_2 with recent bomb ^{14}C measurements. *Global Biogeochem. Cycles*, **21**, GB2015, doi:10.1029/2006GB002784.

Takagaki, N., and S. Komori, 2007: Effects of rainfall on mass transfer across the air-water interface. *J. Geophys. Res.*, **112**, C06006, doi:10.1029/2006JC003752.

Takahashi, T., S. C. Sutherland, C. Sweeney, A. Poisson, N. Metzl, B. Tilbrook, N. Bates, R. Wanninkhof, R. A. Feeley, C. Sabine, J. Olafsson, and Y. Nojiri, 2002: Global sea-air CO_2 flux based on climatological surface ocean pCO_2 and seasonal biological and temperature effects. *Deep-Sea Res. II*, **49**, 1601 – 1622.

Takahashi, T., S. C. Sutherland, R. Wanninkhof, C. Sweeney, R. A. Feely, D. W. Chipman, B. Hales, G. Friederich, F. Chavez, C. Sabine, A. Watson, D. C. E. Bakker, U. Schuster, N. Metzl, H. Yoshikawa-Inoue, M. Ishii, T. Midorikawa, Y. Nojiri, A. Körtzinger, T. Steinhoff, M. Hoppema, J. Olafsson, T. S. Arnarson, B. Tilbrook, T. Johannessen, A. Olsen, R. Bellerby, C. S. Wong, B. Delille, N. A. Bates, and

H. J. W. deBaar, 2009: Climatological mean and decadal change in surface ocean pCO_2 and net sea-air CO_2 flux over the global oceans. *Deep-Sea Res. II*, **56**, 554 – 577.

Thomann, R. V., J. A. Mueller, R. P. Winfield, and C.-R. Huang, 1991: Model of fate and accumulation of PCB homologues in Hudson Estuary. *J. Environ. Eng.*, **117**, 161 – 178.

Tsimplis, M., and S. A. Thorpe, 1989: Wave damping by rain. *Nature*, **342**, 893 – 895.

Tsivoglou, E. C., J. B. Cohen, S. D. Shearer, and P. J. Godsil, 1968: Tracer measurements of stream reaeration. II. Field studies. *J. Water Poll. Control Fed.*, **40**, 285 – 305.

Turk, D., C. J. Zappa, C. S. Meinen, J. R. Christian, D. T. Ho, A. G. Dickson, and W. R. McGillis, 2010: Rain impacts on CO_2 exchange in the western equatorial Pacific Ocean. *Geophys. Res. Lett.*, **37**, L23610, doi:10.1029/2010GL045520.

Ulrich, M. M., S. R. Müller, H. P. Singer, D. M. Imboden, and R. P. Schwarzenbach, 1994: Input and dynamic behavior of the organic pollutants tetrachloroethane, atrazine, and NTA in a lake: A study combining mathematical modeling and field measurements. *Environ. Sci. Technol.*, **28**, 1674 – 1685.

Wanninkhof, R., 1992: Relationship between wind speed and gas exchange over the ocean. *J. Geophys. Res.*, **97**, C5, 7373 – 7382.

Wanninkhof, R., W. Asher, D. T. Ho, C. Sweeney, and W. R. McGillis, 2009: Advances in quantifying air-sea gas exchange and environmental forcing. *Annu. Rev. Marine Sci.*, **1**, 213 – 244, doi:10.1146/annurev.marine.010908.163742.

Wanninkhof, R., W. Asher, R. Weppering, H. Chen, P. Schlosser, C. Langdon, and R. Sambrotto, 1993: Gas transfer experiment on Georges Bank using two volatile deliberate tracers. *J. Geophys. Res.*, **98**, C11, 20,237 – 20,248.

Wanninkhof, R., J. R. Ledwell, and W. S. Broecker, 1985: Gas exchange-wind speed relation measured with sulfur hexafluoride on a lake. *Science*, **227**, 1224 – 1226.

Wanninkhof, R., J. R. Ledwell, W. S. Broecker, and M. Hamilton, 1987: Gas exchange on Mono Lake and Crowley Lake, California. *J. Geophys. Res.*, **92**, C13, 14,567 – 14,580.

Wanninkhof, R., and W. R. McGillis, 1999: A cubic relationship between air-sea CO_2 exchange and wind speed. *Geophys. Res. Lett.*, **26**, 1889 – 1892.

Wanninkhof, R., A. Olsen, and J. Triñanes, 2007: Air-sea CO_2 fluxes in the Caribbean Sea from 2002 – 2004. *J. Mar. Syst.*, **66**, 272 – 284.

Watson, A. J., R. C. Upstill-Goddard, and P. S. Liss, 1991: Air-sea gas exchange in rough and stormy seas measured by a dual-tracer technique. *Nature*, **349**, 145 – 147.

Wilcock, R. J., 1984: Reaeration studies on some New Zealand rivers using methyl chloride as a gas tracer. *Gas Transfer at Water Surfaces*, W. Brutsaert and G. H. Jirka, eds., D. Reidel Publishing Company, Hingham, MA, 413 – 421.

Wu, Y., N. Wang, and K. Rutchey, 2006: An analysis of spatial complexity of ridge and slough patterns in the Everglades ecosystem. *Ecological Complexity*, **3**, 183 – 192.

Yvon, S. A., and J. H. Butler, 1996: An improved estimate of the oceanic lifetime of atmospheric CH_3Br. *Geophys. Res. Lett.*, **23**, 53 – 56.

Zappa, C. J., W. E. Asher, and A. T. Jessup, 2001: Microscale wave breaking and air-water gas transfer. *J. Geophys. Res.*, **106**, C5, 9385 – 9391.

Zappa, C. J., D. T. Ho, W. R. McGillis, M. L. Banner, J. W. H. Dacey, L. F. Bliven, B. Ma, and J. Nystuen, 2009: Rain-induced turbulence and air-sea gas transfer. *J. Geophys. Res.*, **114**, C07009, doi:10.1029/2008JC005008.